Controlling Microbial Colonization and Biofilm Formation Using Surface Topography

Mehdi Kargar

Dissertation submitted to the faculty of the Virginia Polytechnic Institute and State University in partial fulfillment of the requirements for the degree of

Doctor of Philosophy
In
Mechanical Engineering

William A. Ducker, Chair
Masoud Agah
Rafael V. Davalos
Amy Pruden

November 20, 2014
Blacksburg, VA

Keywords: *Pseudomonas aeruginosa*, Colloidal Crystals, Anti-Fouling Coating, Curvature, Cell-Cell interaction

Controlling Microbial Colonization and Biofilm Formation Using Surface Topography

Mehdi Kargar

ABSTRACT

This dissertation introduces assembly of spherical particles as a novel topography-based anti-biofouling coating. It also provides new insights on the effects of surface topography, especially local curvature, on cell–surface and cell–cell interactions during the evolution of biofilms.

I investigated the adhesion, colonization, and biofilm formation of the opportunistic human pathogen *Pseudomonas aeruginosa* on a solid coated in close-packed spheres of polystyrene, using flat polystyrene sheets as a control. The results show that, whereas flat sheets are covered in large clusters after one day, a close-packed layer of 630–1550 nm monodisperse spheres prevents cluster formation. Moreover, the film of spheres reduces the density of *P. aeruginosa* adhered to the solid by 80%. Our data show that when *P. aeruginosa* adheres to the spheres, the distribution is not random. For 630 nm and larger particles, *P. aeruginosa* tends to position its body in the confined spaces between particles. After two days, 3D biofilm structures cover much of the flat polystyrene, whereas 3D biofilms rarely occur on a solid with a colloidal crystal coating of 1550 nm spheres. On 450 nm colloidal crystals, the bacterial growth was intermediate between the flat and 1550 nm spheres. The initial preference for *P. aeruginosa* to adhere to confined spaces is maintained on the second day, even when the cells form clusters: the cells remain in the confined spaces to form non-touching clusters. When the cells do touch, the contact is usually the pole, not the sides of the bacteria. The observations are rationalized based on the potential gains and costs associated with cell-sphere and cell-

cell contacts. I concluded that the anti-biofilm property of the colloidal crystals is correlated with the ability to arrange the individual cells.

I showed that a colloidal crystal coating delays *P. aeruginosa* cluster formation on a medical-grade stainless-steel needle. This suggests that a colloidal crystal approach to biofilm inhibition might be applicable to other materials and geometries. The results presented in appendix A suggest that colloidal crystals can also delay adhesion of *Methicillin resistant staphylococcus aureus* (MRSA) while it supports selective adhesion of this bacterium to the confined spaces.

Acknowledgements

I would like to express my highest gratitude to my adviser, Prof. William Ducker, for trusting me and granting me freedom in research. He has been more than an adviser, and I have benefited from his encouragement, patience, and mentoring. I sincerely thank my committee members: Profs. Amy Pruden, Masoud Agah, Dr. Rafael Davalos for their insightful comments, thought-provoking questions and their support.

I am grateful to my previous advisers: Professors Bahareh Behkam, Mohammad-Hassan Saidi, Ali-Akbar Ghafourian and Mohammad-Ali Dehghan. This was not possible without what I learned from them over the past years. I sincerely appreciate Professor Amy Pruden for giving me access to all her lab facilities for conducting microbial tests. Dr. Pruden was certainly more than a collaborator, and I give my highest regard to her as my mentor. I appreciate Drs. Birgit Scharf, Chang Lu, Steve Melville and Peter J. Vikesland, for providing access to their laboratories and equipment at Virginia Tech. I would like to thank the staff of different offices at Virginia Tech who helped me over the course of this project: Stephen McCartney (NCFL), Kristi DeCourcy (Fralin life science)

I wish to thank my colleagues at both Dr. Ducker's and Dr. Pruden's lab for creating wonderful work environments. I want to especially thank: Jonathan Hittel, Akhil Jindal, Hamoun Khalili Hoseinabad, Timothy Song and Nattasha Srikongyos for their assistance during the research work.

I acknowledge financial support from the David W. Francis and Lillian Francis Scholarship Fund, mechanical engineering department, college of engineering and have

always been Macromolecule and Interfaces institute at Virginia tech.

Last but not least, I don't know what words to use to express my ultimate appreciation, and thanks to my wonderful wife, Atieh. She has been an unlimited source of love, courage, strength, and inspiration. I give my highest gratitude to my parents for their love and for the never-ending sacrifices they made for my success and education. My family, including my in-laws, have always been supportive to me, and I would like to thank them all. To my family, I wish to dedicate this dissertation.

Table of Contents

List of Figures

List of Tables

Chapter 1. Introduction

Bacterial infections are one of the leading causes of human misery, and hospital acquired infections alone are the fourth most common cause of death in the US.[1] In addition to misery and death, these infections are estimated to cost the US approximately $5 billion annually.[2] About 65% of these deaths are caused by infections invading the surface of implants and medical devices.[2] These infections begin with the adhesion of microorganisms to surfaces, continue with the formation of microbial colonies and lead to the formation of biofilms.[2]

1-1. Biofilm formation process

Biofilms are complex microbial communities that form on biotic and abiotic surfaces[2]. Figure 1 shows the biofilm formation process[2]. Biofilm formation starts with interaction of planktonic cells with surfaces. The surfaces might be pre-conditioned due to adsorption of macromolecules, such as protein, which are available in natural environments, e.g blood. Planktonik cells may adhere to the surface however, this adhesion is reversible and bacteria may leave the surface. Under favorable conditions the adhesion may become stronger and irreversible. Irreversible adhesion can lead to formation of small clusters of cells. The small clusters can grow into large micro-colonies by colonal growth, i.e reproduction, or by addition of new cells to the cluster. The combination of individual cells adhered to the surface, small clusters and large micro-colonies create a monolayer aggregation of the cells on the surface. Under favorable conditions, the micro-colonies may evolve into 3D structures, called biofilms, which are composed of cells and excreted molecules, called the matrix.

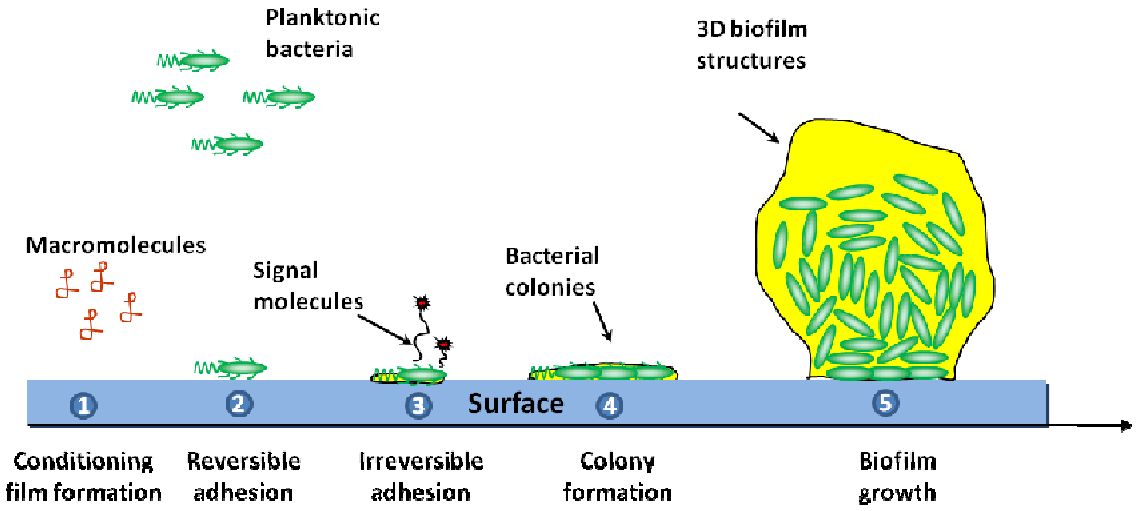

Fig 1-1. Schematic of biofilm formation, adapted from reference[2]. 1. Macromolecules from the environment adsorb to form a "conditioning film". 2. Planktonic bacteria adhere reversibly. 3. Under favorable conditions, the adhesion of bacteria changes from reversible to irreversible and bacteria start forming clusters. 4. Colonies form by growth of clusters, e.g. by reproduction or recruitment. 5. Bacteria form a 3D structure of the biofilm.

1-2. Common antibiofilm formation strategies

The most common medical treatment of device and implant infections is long-term systemic treatment with antibiotics[3]. Antibiotic treatments sometimes fail because of the development of biofilms, which are less responsive to antibiotic treatments,[4] or the presence antibiotic-resistant bacteria such as methicillin-resistant *Staphylococcus aureus* (MRSA).[5] Antibiotic treatments frequently have broad systemic effects on the body, including killing beneficial microbes.[6]

An alternative strategy for reducing the incidence of these infections is to alter the properties of the medical surfaces to delay colonization by bacteria. Chemical

modifications have been widely studied, to either delay adhesion of microbes to the surfaces or kill them upon contact[7]. Surface topography is another property of the surface that can complement the effects of chemistry to reduce fouling[8].

1-3. Engineering surface topography to fight biofilms

Antifouling surfaces with topographical features are observed widely in nature, [9-12] and this has inspired the preparation of artificial surface patterning to prevent the adhesion of bacteria[13-30]. Figures 1-2 show some examples of the topographical features on natural antifouling surfaces. Figure 1-2 shows the surface topography of *Mytilus edulis* (blue mussle), *Scyliorhinus canicula* (small spotted catshark), *Cancer pagurus* (brown crab). The replicate cast in epoxy resin of the topographical features of the mentioned organisms could reduce the fouling for three to four weeks.[12]

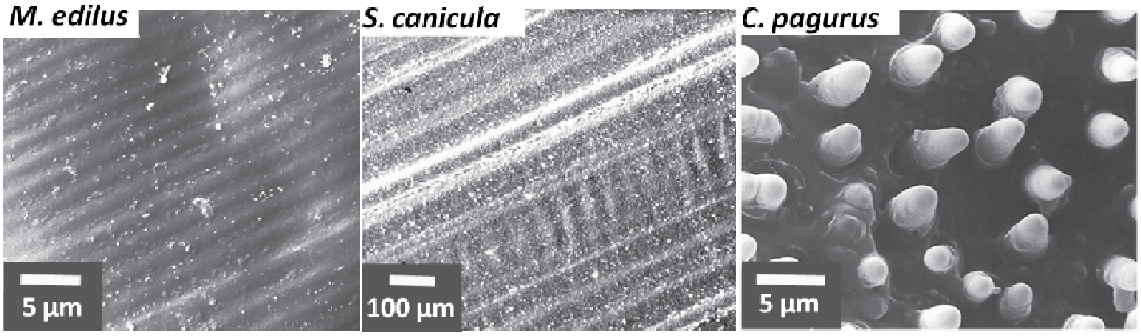

Fig. 1-2. Scanning electron micrograph of the surface topography of natural antifouling surface of marine organisms: *Mytilus edulis* (blue mussle), *Scyliorhinus canicula* (small spotted catshark), *Cancer pagurus* (brown crab). The image reprinted from reference 12 with permission from the publisher Taylor & Francis.

Chung *et al.*[15] prepared a surface that mimicked the topography of shark skin. This surface contained protrusions about 4-16 µm in length, 2 µm in width and 3 µm in

height spaced by 2 µm (Fig. 1-3). Chung *et al.* showed that although these features did not prevent adhesion of bacteria, the formation of biofilms was greatly delayed. The authors attributed this effect to the "physical obstacle" presented by the protrusions.

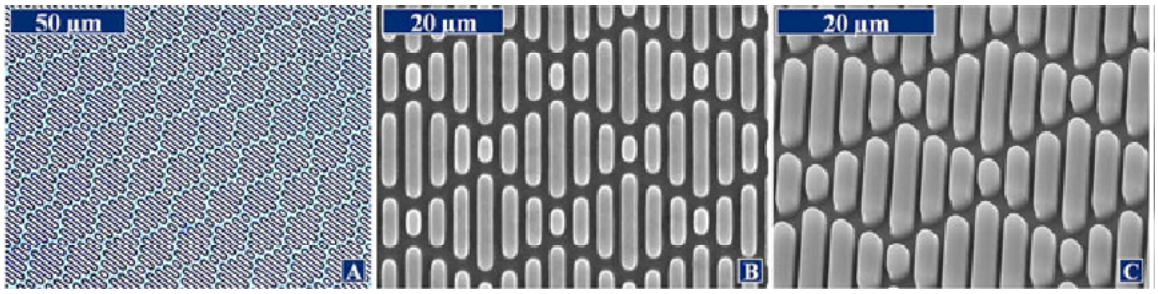

Fig. 1-3. The Sharklet topographical features created by Chung et. al[15]. A) light micrograph from top-down view, B) Scanning electron micrograph, and C) Scanning electron micrograph taken at 35°. The image reprinted with permission from 15. Copyright 2007, American Vacuum Society.

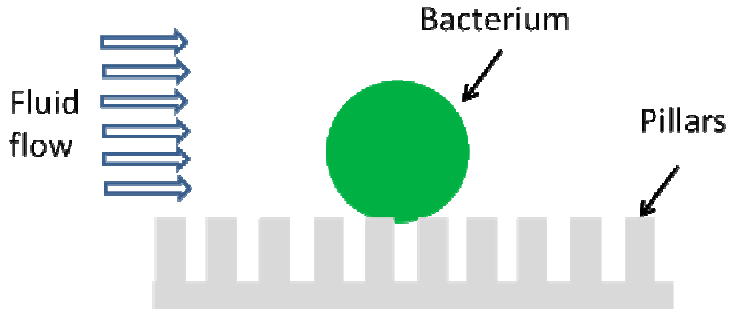

Fig. 1-4. Schematic of a spherical bacterium sitting on top of the pillars. When a bacterium sits on top of the pillars, it loses some contact points with solids due the gaps available between the pillars. Therefore the adhesion to the top of the pillars may be less strong than when bacterium adheres to a flat surface.[30] Therefore the bacteria may be washed off from the surface due to the shear forces applied by fluid flow.

Xu and Siedlecki[30] studied adhesion and colonization of *Staphylococcus aureus*

and *Staphylococcus epidermidis* on flat and pillar textured poly(urethane urea). They observed reduced adhesion and delayed colony formation on textured surfaces. They attributed their observation to the potential effects of the hydrodynamic shear forces present in their experiments. Xu and Siedlecki,[30] hypothesized that if texturizing the surfaces reduces the available contact area between the cells and the solid surface, it can support ease of cell removal and delay biofilm formation (Fig. 1-4).

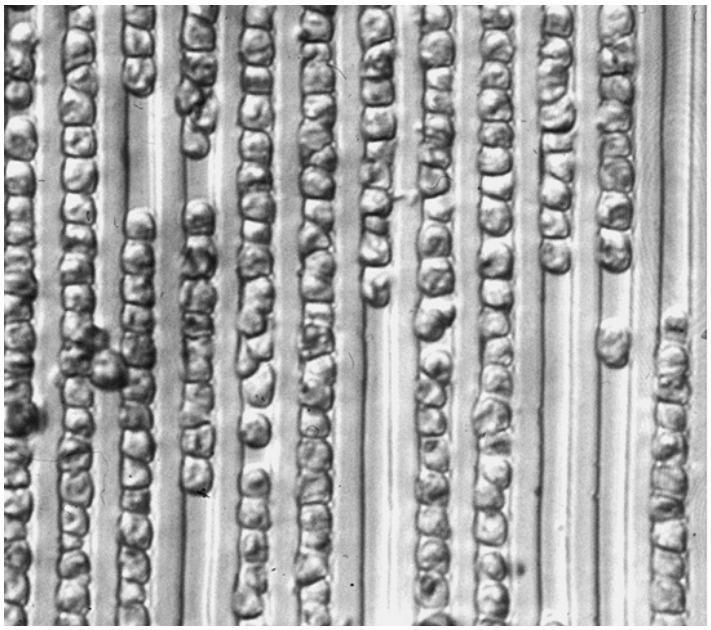

Fig. 1-5. When interacting with ridges, zoospores of the green fouling alga *Enteromorpha* prefer to stay inside the channels[14]. Each channel is 5 μm in width and depth. The image reprinted from reference 14 with permission from the publisher Taylor & Francis.

When studying interactions of microorganisms with topographically engineered surfaces, several researchers observed selective adhesion of variety microorganisms to the specific binding sites on topographically engineered surfaces. For example, studying the interaction of marine microorganisms with the textured surfaces, Callow et. al.[14], suggested that cells are trying to increase the number of attachment points to the surface.

Therefore, the binding sites which offer more attachment points are preferred for adhesion (Fig. 1-5). . Callow et. al[14] suggested that their observations could be related to the concept of surfaces energy. They hypothesized that making further contact areas with the surface will result in more gain in energy of adhesion.

Previous work suggests that both strain specificity and motility are important factors in selectivity.[13, 14, 16-22, 24-26, 29] With respect to motility, Scardino *et al*.[24] compared the interactions of motile and non-motile marine organisms with topographically engineered surfaces and reported that whereas the number of adhered motile cells depended on the topography, the number of adhered non-motile cells did not.

1-4. Biofilm formation by *Pseudomonas aeruginosa on solid surfaces*

1-4-1. Biofilm formation by *P. aeruginosa* on flat surfaces

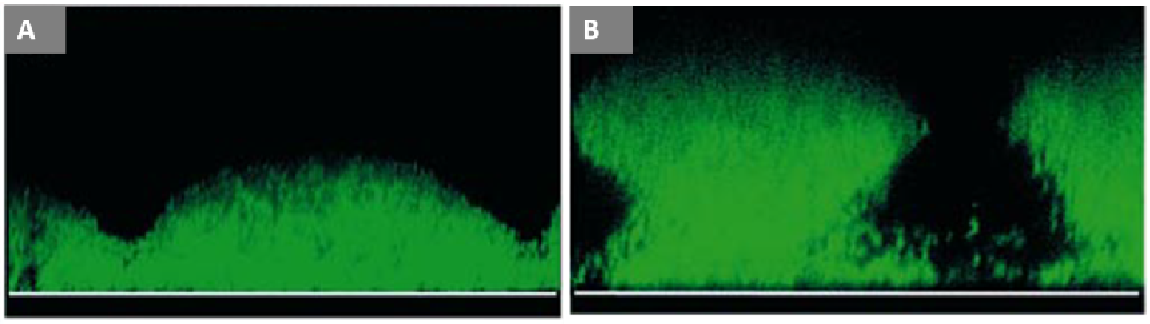

Fig 1-6. Confocal microscopic images of A) early stage and B) mature mushroom shape biofilm formed by *Pseudomonas aeruginosa*[31]. The growth media used in the experiments is similar to the media used in my experiments. Reprinted by permission from Macmillan Publishers Ltd: [Nature] (reference 31) , copyright (2002)

I used *Pseudomonas aeruginosa*, a rod shape, Gram-negative and motile bacteria as the model microorganism. *P. aeruginosa* it is an opportunistic human

pathogen that exists in biofilms in hospital environments.[32] Live imaging of the biofilm formation of *P. aeruginosa* on flat solid surfaces cells suggest that after cells adhere to the surface, some of them may remain sessile while the rest will move on the surface[33]. To form micro-colonies the surface motility should be down-regulated[34]. Growth of a colony occurs using two mechanisms colonal growth or cell aggregation, adhesion of a new cell to a colony[34, 35]. The shape of the biofilm formed by *P. aeruginosa* depends on the carbon source used in the biofilm formation assays[33, 34, 36]. Using glucose as the carbon source, in particular the nutrient source used in this work[31, 35], will support formation of mushroom-shape 3D structures in *P. aeruginosa* biofilm (Fig. 1-6)[31, 33-36].

1-4-2. Effects of surfaces topography on *P. aeruginosa* - solid surface interactions

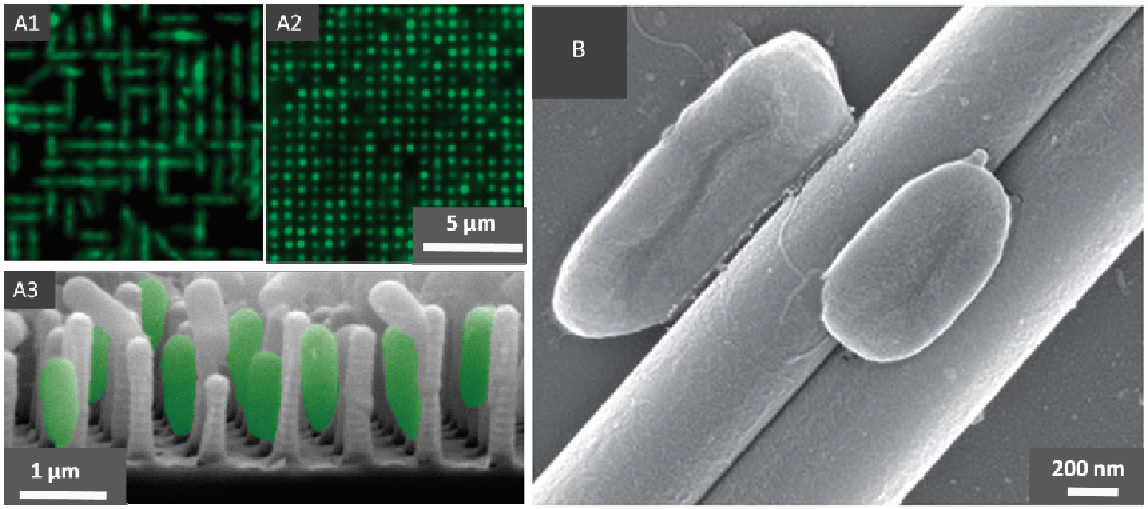

Fig. 1-7. Colored SEM image (A1) and fluorescent (A2 and A3) of *P. aeruginosa,* PA14 interacting with pillars[18]. Figure A1 and A2 are showing that cells aligned themselves in response to the changes in spacing between nearby pillars[18]. Reprinted with permission from reference 18. Copyright (2010) American Chemical Society B) High magnification SEM image of *P. aeruginosa,* PAO1 aligned with polystyrene nanofibers[22]. Reproduced by permission of The Royal Society of Chemistry.

There are some previous studies on adhesion of *P. aeruginosa* to topographical engineered surface. However, to the best of my knowledge, the biofilm formation of *P. aeruginosa* on topographically engineered surfaces is not studied yet. The previous studies suggest when adhering to topographical features, *P. aeruginosa*, is capable of both select the specific binding sites and configure the alignment of its rod shape body[17, 18, 21, 22]. In particular, Hochbaum and Aizenberg[18] studied interactions of bacteria with submicron-size pillars, and concluded that when interacting with the spacing between the pillar, each cell selected an alignment that provided it with greater contact area with the surface (Fig. 1-7 A).

Kargar *et al.*[22] investigated the adhesion of *P. aeruginosa* to fibrous surfaces at a single cell level. They showed that *P. aeruginosa* selectively binds to specific locations of the fibrous surfaces, and gave insights into the action of local surface curvature on hindering microbial adhesion (Fig. 1-7 B). Kargar *et al*[22] explained that in order to increase their contact area with curve surfaces, the cells have to curve away. Therefore adhesion to more curved structures should be less favorable as it requires more deformation. They based their discussions on a balance between adhesion energy and deformation energy, following the work on vesicle adhesion described by Seifert and Lipowsky.[37]. The total free energy of adhesion by Eq. 1-1:

$$\Delta G_{adhesion} = -\Delta G_{contact} + \Delta G_{tension} + \Delta G_{bending} + \Delta G_{pressure} \quad (1\text{-}1)$$

$-\Delta G_{contact}$ represents the gain in adhesion process due to making contact with the surface. $\Delta G_{contact} = wA_c$ where w is the specific adhesion energy (J/m^2) and A_c is the contact area (m^2) between vesicle and the surface. $\Delta G_{tension}$ is the cost associated

with increased area of vesicle (ΔO, m^2) which is under tension (α, J/m^2). $\Delta G_{tension} = \alpha \Delta O$. $\Delta G_{bending}$ is the energy cost associated with bending of the membrane. The bending deformation of a thin membrane is determined by its mean curvature: $H = \frac{1}{R_1} + \frac{1}{R_2}$.where R_1 and R_2 are the principle radii of curvature (m) of the surface. If the thickness of the vesicle membrane is small compared to its radius then the following approximation may be used to calculate bending energy[38] $\Delta G_{bending} = {}^{1}/_{2\kappa} \iint H^2 \mathrm{d}O$ where κ is two-dimensional bending modulus of the membrane (J). $\Delta G_{pressure}$ is the potential cost associated with increase in the volume of the system (ΔV, m^3). $\Delta G_{pressure} = p\Delta V$ where p is the vesicle pressure (Pa). Although equation 1-1 is very complex and can be only solved for very simple cases,[38] but, In principle, it can be used to predict both adhesion state and final shape of a vesicle contacting a surface[38]. Therefore, it was suggested that this model may be used as a useful tool to qualitatively interpret the results observed during the adhesion of microbial cells to the topographically engineered surfaces[22].

Kargar *et al.*[21] observed that *P. aeruginosa* PAO1: wild type *P. aeruginosa* selectively attached to specific binding sites on fibrous surfaces whereas the non-motile pila mutants, (lacking type IV pili, used for surface motility) lacked selectivity (Fig. 1-8).

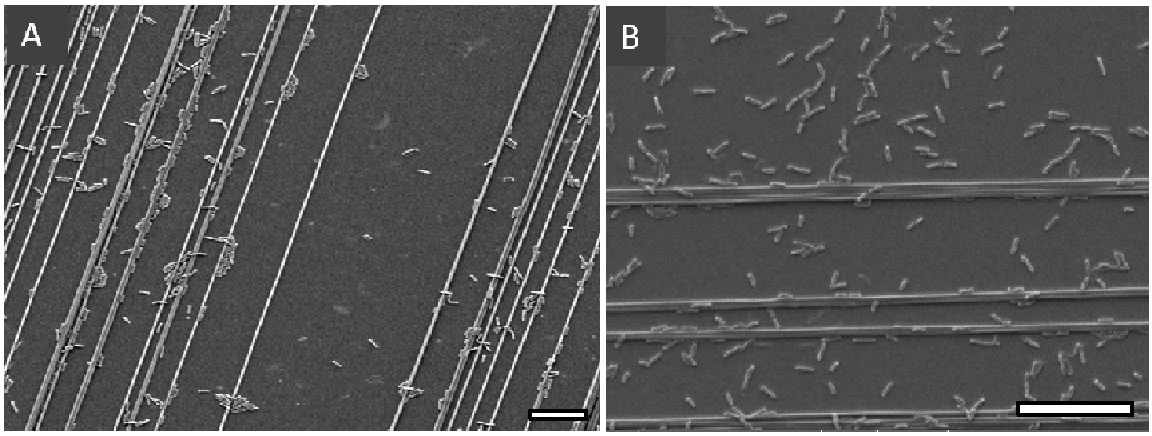

Fig. 1-8. SEM images of *P. aeruginosa,* PAO1, adhering to the polystyrene nanofibers. A) wild type B) pila mutants (lacking type IV pili, used for surface motility)[21]. Scale bars represent 15 μm.

1-5. Hypothesis

My hypothesis is that coating surfaces with assembly of microspheres can delay biofilm formation. We based this hypothesis on the potential effects of the local curvature on the microbial adhesion to the surfaces described by Kargar et. al.22 We selected spheres for this study because they have constant curvature at every point.

1-6. Colloidal crystals as assembly of particles

A regular arrangement of colloidal particles is also called a "colloidal crystal", and in this dissertation I use the term colloidal crystals to refer to a *monolayer* of close packed spheres (shown in Fig. 3-1). The principal advantages of colloidal crystals to prevent microbial colonization are: (1) they can be used to coat a broad range of surfaces, regardless of their chemistry;[39, 40] (2) they can coat surfaces with complex geometries, for example curved and non-planar surfaces;[39-41] (3) they can be used to produce a broad

range of feature sizes (larger than 50 nm);[13] (4) they can be produced on large areas at low cost in a short time without to the requirement of sophisticated facilities such as a clean room;[41] and (5) they can provide surfaces with well-defined curvatures on the nano-micro scale[42]. Here I examine the effects of polystyrene colloidal crystal coatings (diameter 200 nm–1600 nm) on all stages of biofilm formation from adhesion to formation of 3D structures. Polystyrene (PS) spheres of various sized are commercially available. All PS samples were exposed to fetal bovine serum before bacterial experiments. This leaves an adsorbed layer of protein, which is common for surfaces in biological systems.

1-7. Outline of dissertation

The dissertation is structured into five chapters. The first chapter provides introduction and summaries the previous works. In the second chapter, I provide the general experimental procedures practiced during the experiments. The manufacturing process is also explained in second chapter. The third chapter discussed the effect of particle size on adhesion and early stage colony formation of *P. aeruginosa*. In that chapter I also show that colloidal crystals can delay bacterial adhesion on materials other than polystyrene. The results presented in the third chapter of dissertation are published in the Journal of Materials Chemistry B with professors Amy Pruden and William Ducker as co-authors. The Fourth chapter describes colony growth and 3D biofilm formation. In the fifth and the final chapter I summarize the findings, make conclusions and make suggestions for future works. The results of the chapter four of dissertation will also be submitted to Journal of Materials Chemistry B . The co-authors of this paper are Mr. Hamoun Kahlili Hoseinabad, Professor Amy Pruden and Professor William

Ducker. The dissertation also have two appendices providing supporting data about potential of colloidal crystals in delaying adhesion of other bacteria such methicillin resistant *Staphylococcus aureus* (MRSA) and potential improvements for other materials such as PTFE catheters.

Chapter 2. Materials and General Experimental Methods

In this chapter, I will describe general experimental procedures used during the thesis. The specific procedures that were designed and used for specific chapters will be explained in the relevant chapter.

2-1. Chemicals

The following chemicals and regents were all obtained from Fisher scientific (Pittsburg, PA): acetone (HPLC grade), sulfuric acid (18M), tryptic soy broth (TSB) powder, tryptic soy agar (TSA) powder and Hyclone fetal bovine serum (FBS). TSA plates were prepared by adding 1 liter of DI water to 40 g of TSA. TSB media was prepared by adding 1 liter of water to 30 g of TSB powder. The other chemicals used in the experiments are: Hydrogen peroxide, 30% in water (LabChem Inc., Zelienople, PA), USP grade 200 proof ethanol (Decon Laboratories, King of Prussia, PA) and 10% EM grade glutaraldehyde (Electron Microscopy Sciences, Hatfield, PA) Sodium dodecyl sulfate (SDS) and potassium nitrate were purchased from Sigma-Aldrich (St. Louis, MO). All PS spheres have been purchased from Bangs laboratory incorporation (Fishers, IN). The flat sheets of PS film that were used as control flat surfaces were purchased from Goodfellow (Coraopolis, PA). Deionized (DI) water used in the experiments had resistivity 18.2 MΩ cm at 25 °C. Diluted TSB, Ethanol and glutaraldehyde have made by mixing DI water and the original chemical with the appropriate ratio. L7007 live dead assay kit was purchased from Invitrogen (Grand Island, NY).

2-2. Manufacturing the colloidal crystal monolayers

Several methods for manufacturing colloidal crystal films are described in the literature.[43] As shown in Fig. 2-1A, my films were prepared by first depositing particles at the liquid–gas interface, and then pulling a solid from within the solution out into the air through the interface (emersing).[39-41, 44]

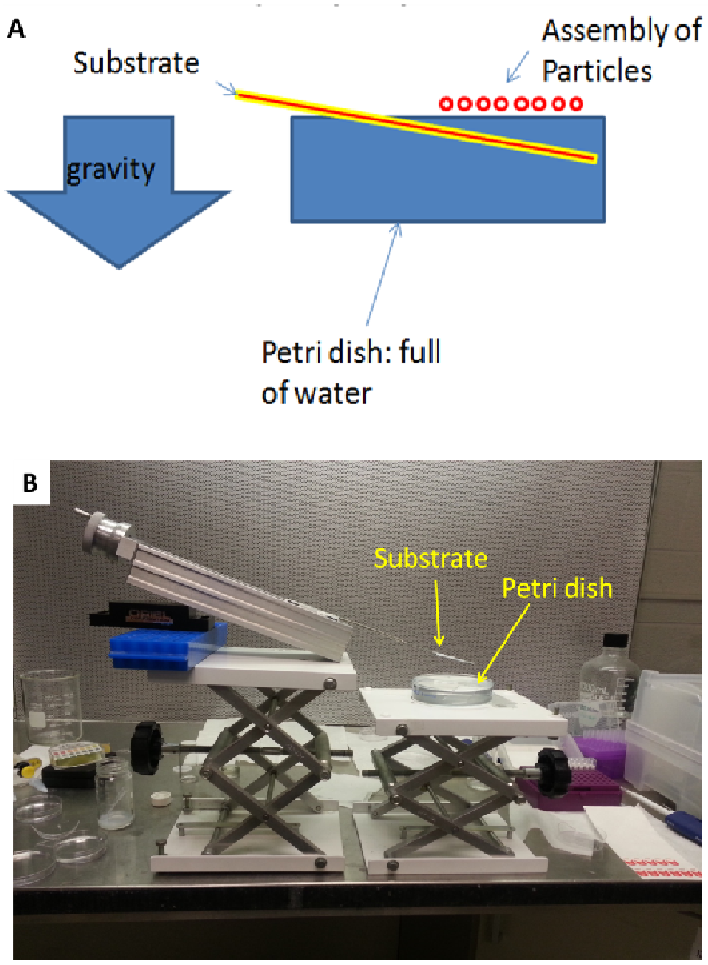

Fig. 2-1. A) The principle behind the manufacturing technique used in this dissertation: Particles assembled at water-air interface and deposited on substrate using gravitional deposition. B) the photograph of the set-up used to texturize surfaces with assembly of particles.

Figure 2-1B shows a photograph of the set-up that designed and used in this

work. Here I will refer to the solid underneath the particles as the "substrate" and the colloidal crystal film plus substrate that is subsequently used for bacterial testing as the "sample".

I have adopted the specific procedure from Lu and Zhou[44]. Briefly, the particles were re-suspended in 1:1 ethanol–DI water solution and deposited at the water/air interface by flowing the particle suspension down a glass slide. The slides were cleaned using consecutive washes with acetone, ethanol, DI water followed by nitrogen drying and cleaning by Piranha solution (1/3 H_2O_2/H_2SO_4). The particles were then deposited on the substrate by emersing the substrate though the interfacial particles. In most cases the substrate was a flat sheet of polystyrene. As recommended by Lu and Zhou,[44] I have added a small amount of SDS to the suspension to facilitate the formation of the closed pack structures. After formation of the colloidal crystal, I heated the sample at 95°C for 110 min. This heating close to the glass transition temperature increases the area of contacts and thus strengthens bonds between particles and between the particles and the substrate.

This method enabled manufacture of colloidal crystal from various particle sizes, but the reproducibility was low. Our original substrates were 100 mm circles of a 0.125 mm thick PS film. After deposition of the colloidal crystal, I cut 1.5 × 0.5 mm^2 rectangular samples with high quality colloidal crystal for our biological test assay. The quality of the film was always characterized using a combination of the diffraction patterns from a laser, based on the Bragg's law[45] and scanning electron microscopy (SEM) imaging.

2-3. Characterization of substrates, spheres and samples

XPS measurements were performed on a Phi Quantera SXM with a monochromatic Al Kα X-ray source (1486 eV). All of the XPS measurements were obtained at a 45^{o} takeoff angle from a 200 μm diameter spot. The wide energy scans were acquired with a 280 eV pass energy in 15 sweeps at 1 eV step size and narrow energy scans were acquired at pass energy 26 eV with 10– 40 sweeps depending on the element at 0.1 eV step size.

Zeta potential measurements of colloidal spheres were performed with a Zetasizer Nano ZS (Malvern, Worcestershire, United Kingdom). The zeta potential was obtained from the mobility using the appropriate correction term for the ratio between the radius and Debye-length[46]. The zeta potential of the flat PS film and particle-coated surfaces was determined using a SurPASS Electrokinetic Analyzer (Anton Paar GmbH, Graz, Austria). The surfaces were washed with water, then ethanol, and then dried in stream of pure nitrogen. The solvent for all zeta potential measurements was 0.05 mM KNO_3 solution.

The roughness of the flat PS substrates was measured using atomic force microscopy (AFM) (MFP3D, Asylum Research, Santa Barbara, CA) using ORC8 cantilevers (Bruker, Camarillo, CA) with a nominal spring constant of 0.7 N/m in contact mode.

2-4. Preparation of samples for biological assays

All samples were washed with DI water at 37 $^{\circ}$C in a rotary shaker (100 rpm) for

1 hour and stored in Petri dishes. Before biological tests, the samples were washed with 100% ethanol and sterilized by soaking in 70% ethanol following by three washes with autoclaved DI water. In order to mimic the conditioning film that samples will experience in a biological environment all samples were submerged under 2ml FBS in wells of 12 well plates and incubated at 37^{o}C overnight, following a protocol for testing catheters.[47] Negative control experiments (i.e. with no bacteria) were conducted by transferring some of the FBS-treated samples to a new 12 well plate and incubating them under sterile TSB for a day. Samples that were coated in FBS had a water contact angle <10°.

2-5. Bacterial culturing

Pseudomonas aeruginosa (ATCC^{R} 47085^{TM}), PAO1, was used as the model microorganism in a Center for Disease Control (CDC) reactor (BioSurface Technologies Co., Bozeman, MO). I followed the standard protocol developed by Goeres *et al.*[48] and recommended by the manufacturer of the biofilm reactor with some minor modifications.

A 1.5% TSA plate was streaked using bacteria from -80^{o}C stock and incubated overnight at 37^{o}C. 100 ml of autoclaved culture media (1% TSB) was transferred to a sterile 300 ml flask, inoculated using a single colony from the TSA plate and incubated for 24 hours at 37 ^{o}C on a rotary shaker (170-180RPM). These conditions consistently resulted in $OD_{600} \approx 0.06$. Optical density (or absorbance) is defined as ratio of the amount of radiation falling upon the bacterial suspension to the amount of radiation transmitted through the bacterial suspension. Optical density of bacterial suspension correlates with the number of the cells available inside the solution.

2-6. One day retention assay using CDC reactor

The samples were mounted on the rods of CDC reactor, 323.3 ml of 1% TSB were added, and then 1.7 ml of bacterial culture was used to inoculate the reactor. A dynamic retention assay was conducted for 24 hours n which the baffle of the reactor was stirring at 50 RPM (Fig. 2-2). The experiments were conducted in constant room temperature at 37^{o}C. The filter allowed the exchange of bacteria between reactor and outside environment. During the one day experiments, both inlet and outlet were blocked and it was no flow through of media. To estimate the shear stress due to rotation of the baffle at the surface of the samples, I have followed the method of Buckingham-Meyer *et al.*[49] and used the equations for the shear forces between concentric cylinders where the inner cylinder rotates. This suggests that 50 RPM baffle speed results in a shear stress of about 0.004 N/m^2 at the surface of the sample, which is low compared to the shear rate in other studies.[30]

2-7. Light microscopy imaging of the samples

Light microscopy was used to image the cells in the hydrated state (under water), and after dehydration. Samples were washed with autoclaved DI water (as for SEM) and then fixed in 2.5% glutaraldehyde in water at 4^{o}C. For fluorescent microscopy, the cells stained with a mixture of propidium iodide and SYTO®9 nucleic acid stain. For all imaging, samples were attached to the bottom of glass-bottom petri dishes using PDMS.

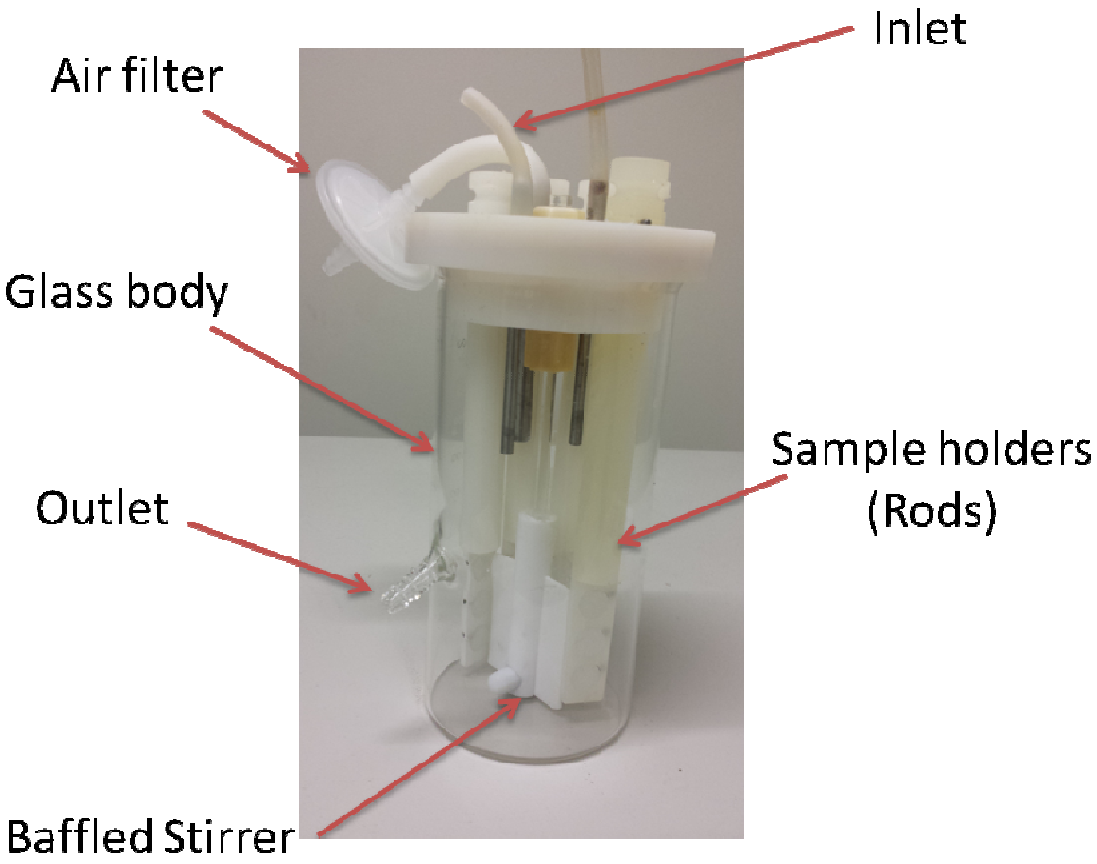

Fig. 2-2. A typical CDC reactor with all components. During the one day experiments, it was no flow thought the inlet and outlet and they were seal blocked. The air filter allows exchange of air between reactor environment and the outside. Magnetic baffle stirrer stirs due to presence of a stirring plate underneath the reactor and provides the fluid flow. Rods used to hold the sample inside the reactor.

Chapter 3. Preventing Bacterial Colonization Using Colloidal Crystals[1]

Abstract

We[2] investigated the adhesion and colony formation of *Pseudomonas aeruginosa* PAO1 on a solid coated in close-packed spheres of polystyrene. The objective was to determine the effect of surface topography on the early stages of biofilm formation. Solids were pretreated with serum and then exposed to bacteria under low shear for one day in a center for disease control biofilm reactor. Whereas flat sheets were covered in large colonies after one day, a close-packed layer of 630–1550 nm monodisperse spheres prevents colony formation. Moreover, the film of spheres reduces the density of *P. aeruginosa* adhered to the solid by an average of 80%. Our data show that when *P. aeruginosa* adheres to the spheres, the distribution is not random. For 630 nm and larger particles, *P. aeruginosa* tends to position its body in a 2-fold site. We rationalize the selectivity on the basis of energy minimization for adhesion: sites differ in the deformation needed to achieve a given contact area. We rationalize the inhibition of colonization by the 630–1550 nm spheres in terms of the lack of adjacent favorable positions for bacteria. A close-packed layer of polystyrene spheres also delays colony formation on a medical-grade stainless-steel needle over a period of one day. This suggests that a colloidal crystal approach to biofilm inhibition might be applicable to a variety of materials and geometries.

[1] This chapter is published and cited as reference 50. M. Kargar, A. Pruden and W. A. Ducker, *Journal of Materials Chemistry B*, 2014, **2**, 5962-5971.
[2] "We" refers to me and my co-authors in this work

3-1. Introduction

Bacterial infections are one of the leading causes of human misery, and hospital acquired infections alone are the fourth most common cause of death in the US[1]. About 65% of these deaths are caused by infections invading the surface of implants and medical devices[2]. These infections begin with the adhesion of microorganisms to surfaces, continue with the formation of microbial colonies and lead to the formation of biofilms[22]. In addition to misery and death, these infections are estimated to cost the US approximately $5 billion annually.[2]

The most common medical treatment of device and implant infections is long-term systemic treatment with antibiotics[3]. Antibiotic treatments sometimes fail because of the development of biofilms, which are less responsive to antibiotic treatments,[4] or the presence antibiotic-resistant bacteria such as methicillin-resistant *Staphylococcus aureus* (MRSA)[5]. Antibiotic treatments frequently have broad systemic effects on the body, including killing beneficial microbes.[6]

An alternative strategy for reducing the incidence of these infections is to alter the properties of the medical surfaces to delay colonization by bacteria. Chemical modifications have been widely studied, to either delay adhesion of microbes to the surfaces or kill them upon contact[7]. Surface topography is another property of the surface that can complement the effects of chemistry to reduce fouling[8] further.

Antifouling surfaces with topographical features are observed widely in nature,[9-11, 20] and this has inspired the preparation of artificial surface patterning to prevent the adhesion of bacteria. For example, Chung et al[15] prepared a surface that mimicked the

topography of shark skin. This surface contained protrusions about 4-16 μm in length, 2 μm in width and 3 μm in height spaced by 2 μm. Chung et al. showed that although these features did not prevent adhesion of bacteria, the formation of biofilms was greatly delayed. The authors attributed this effect to the "physical obstacle" presented by the protrusions.

A number of other studies have examined the effect of topography on bacterial interactions with surfaces.[13, 15, 17, 19, 22, 29, 30, 51, 52] For example, Hochbaum and Aizenberg[18] studied interactions of bacteria with submicron-size pillars, and concluded that when interacting with the spacing between the pillar, each cell selected an alignment that provided it with greater contact area with the surface. Kargar et al.[22] investigated the adhesion of *P. aeruginosa* to fibrous surfaces at a single cell level. They showed that *P. aeruginosa* selectively binds to specific locations of the fibrous surfaces, and gave insights into the action of local surface curvature on hindering microbial adhesion.

One of the major barriers to advancing topographical-based antifouling technologies is fabricating the structure. Well-organized structures within the size range of bacteria (submicron-micron) are needed over the exposed area of a medical device. Most techniques used in the past are constrained by a limited range of suitable materials and/or the requirement of sophisticated facilities, which adds greatly to the expense of manufacturing. The purpose of this study was to examine the use of an adsorbed monolayer of close-packed spheres as a topographical inhibitor of bacterial adhesion and colony formation.

A regular arrangement of colloidal particles is also called a "colloidal crystal",

and in this paper we use the term colloidal crystals to refer to a *monolayer* of close packed spheres. The principal advantages of colloidal crystal to prevent microbial colonization are: (1) they can be used to coat a broad range of surfaces, regardless of their chemistry;[39, 40] (2) they can coat surfaces with complex geometries, for example curved and non-planar surfaces;[39-41] (3) they can be used to produce a broad range of feature sizes (larger than 50 nm);[13] (4) they can be produced on large areas at low cost in a short time without to the requirement of sophisticated facilities such as a clean room;[41] and (5) they can provide surfaces with well-defined curvatures in nano-micron scale[42]. Here we examine the effects of polystyrene colloidal crystal coatings (diameter 200 nm–1600 nm) on bacterial colonization of polystyrene (PS). PS spheres of various sized are commercially available. All PS samples were exposed to fetal bovine serum before bacterial experiments. This leaves an adsorbed layer of protein, which is common for surfaces in biological systems. We use *Pseudomonas aeruginosa*, a rod shape, Gram-negative and motile bacteria as our model bacterium, it is an opportunistic human pathogen that exists in biofilms in hospital environments.[32]

3-2. Experimental

Materials and the general experimental methods have been explained in Chapter 2. Here I explain the procedures which are specifically used in this chapter.

3-2-1. Data analysis and statistics

SEM images were analyzed quantitatively. Only the 0.5×0.5 mm^2 square-shaped area in the middle of the 1.5×0.5 mm^2 area of the sample was used, so as to avoid edge effects. A standard grid containing the positions for counting was placed over

a low magnification image (35×) in which the bacteria were too small to be imaged. This prevented any potential bios when capturing the images. Images were then captured at each of 20 positions on this standard grid, and the number of bacteria per unit area was obtained by manual counting and then averaged. Cell counting was assisted by ImageJ software,[53] and the convergence of the counting results was monitored during the counting process. For most particle samples, convergence occurred after counting 8–10 samples, but for the flat surfaces further counting was required. The magnification of the images used in counting process was 3500× for flat samples and 6000× for colloidal crystals.

3-2-2. Light microscopy imaging of the samples

An Olympus 1X81microscope and Slidebook 5 software was used to capture light microscopy images used in this chapter.

3-3. Results

3-3-1. Characterization of flat and colloidal-crystal-coated surfaces

3-3-1-A. Chemical characterization of the spheres and flat sheets.

To isolate the effect of topography on the formation of bacterial colonies, we minimized the variation in chemistry between samples. For this purpose, we used one chemistry of material, polystyrene (PS), for all topographical studies, and all polystyrene particles were sourced from the same manufacturer. Possible variation in chemistry was examined using XPS and zeta potential measurements. There is a more silicon contamination on the flat surface (~0.5%) than in the particles (0–0.1%), but otherwise the elemental composition of all materials is very similar, and less than or equal to the variation between repeat measurements on the same sample (See Table 3-1). The zeta

potentials in 0.05 mM KNO_3 solution (Table 3-2) were all negative.

There was only a small variation in the zeta potential of the particles (~20%), but the flat sheet had a lower potential than the particles, despite the similarity in the chemistry as measured by XPS. This difference may be explained in part due to different techniques used (electrophoresis vs streaming potential). After noting this possible difference, we created additional flat samples in which the colloidal crystal on a flat glass substrates was sintered by heat treatment at 120°C (higher than the glass transition temperature of PS) for 12 days followed by heat treatment at 140°C for one day, by which time the spheres Ostwald ripened into flat sheets. We refer to these as *flattened* samples. When comparing the flattened samples to a colloidal crystal, we were even more confident that the samples had the same chemistry. Further, we noted that the flattened samples and the flat samples had the same water contact angle of 91°.

Table 3-1. Percentage of element on the surface of each sample surface measured by XPS.

		Sample Set 1		
Topography	**C_{1s}***	**O_{1s}**	**Si_{2p}**	**S_{2p}**
Flat	94.9	4.6	0.5	0.0
220 nm	95.4	4.5	0.1	0.1
450 nm	95.2	4.6	0.0	0.2
630 nm	95.3	4.6	0.1	0.1
830 nm	95.3	4.5	0.1	0.1
925 nm	95.2	4.7	0.0	0.1
1550 nm	95.0	4.8	0.0	0.2
		Sample Set 2		
Topography	**C_{1s}**	**O_{1s}**	**Si_{2p}**	**S_{2p}**
Flat	98.1	1.5	0.4	0.0
220 nm	99.2	0.7	0.1	0.0
450 nm	98.8	1.1	0.0	0.1
830 nm	98.7	1.2	0.0	0.1

*Columns titles describe the electron orbital used to determine the element.

Table 3-2. Zeta Potential of Particles, substrates and samples. (Average of 20 measurements.)

Diameter (nm)	Zeta potential (mV)	St. De. (mV)
220	-77	7
450	-73	11
630	-79	8
830	-88	8
925	-89	8
1550	-94	13
flat	-54	4

3-3-1-B. Topographical characterization of the flat surfaces

AFM imaging showed that the PS sheet had no features on the scale of 50–1000 nm, thus the PS sheet was able to serve as a control that had no features on the scale of the bacterial dimensions. The measured rms roughness was 1.5 nm over an area of 625 μm^2, so the sheeting was also smooth. In other words, the feature size was much smaller than the smallest particle size (220 nm) used to make the colloidal crystal samples.

3-3-1-C. Formation of close-packed films.

An example of a colloidal crystal that was deposited on a polystyrene Petri dish is shown in Figure 3-1. The optical image shows opalescence typical of colloidal crystals (Figure 3-1A), and irregularly shaped domains that are of the order of 5 mm in size. An SEM image indicated hexagonal close-packed ordering of the 450 nm particles (Figure 3-1B), and the diffraction pattern from a 532 nm laser (spot size ~ 1mm) confirmed (a) the existence of domains of a size exceeding the laser spot size, and (b) that the hexagonal ordering of the particles persisted over several diameters (Figure 3-1C). The contact angle of the colloidal crystals was about the same as for the flat sample, ≈90°. After pretreatment with FBS, all the polystyrene surfaces had a low contact angle, < 10°.

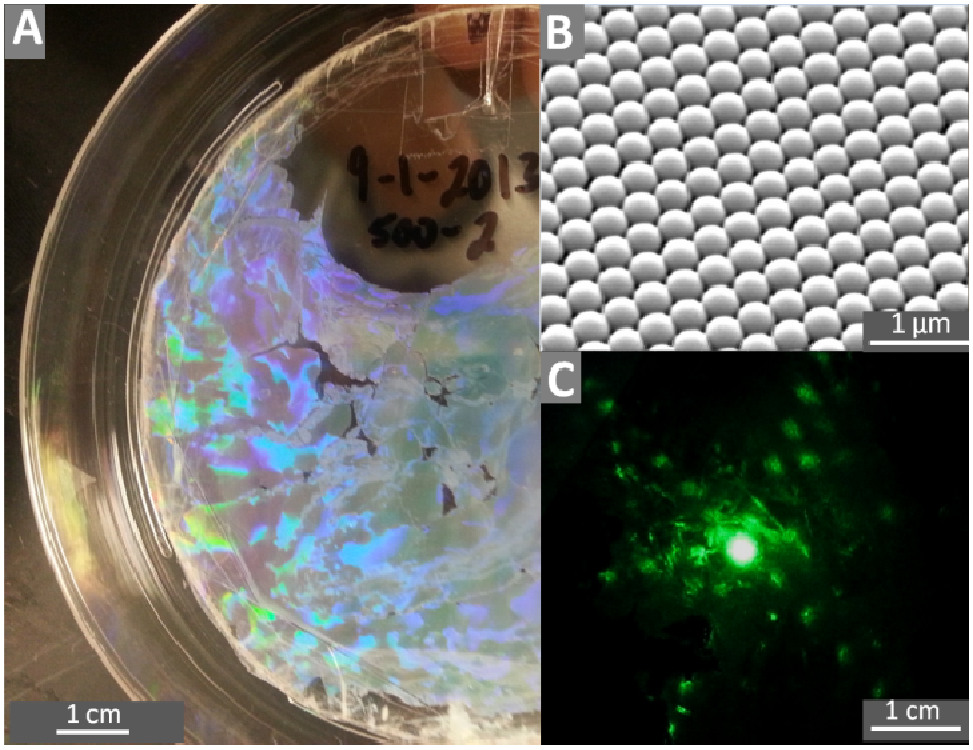

Fig. 3-1. A) 100 mm plate covered in a 450 nm colloidal crystal; B) SEM image of 450nm colloidal crystal, C) Diffraction pattern from the plate produced by a 532 nm laser.

3-3-1-D. Robustness of colloidal crystal films

SEM imaging showed that the colloidal crystals remained intact during the period of the experiments, even though they were washed using a rotary shaker (DI water, 100 rpm, 37°C), rinsed with water or ethanol using a pipette, and during the biological experiments, subjected to a shear stress of ~0.004 N/m2.

3-3-2. Effect of sphere coating on bacterial adhesion and colony formation

3-3-2-A. Preventing formation of microbial colonies

Flat PS samples and colloidal crystal PS substrates were exposed to bacteria in a CDC reactor for 24 hours in TSB medium (300 mgL^{-1}), after pre-treatment with FBS. Figure 3-2 compares the distribution of bacteria, as shown by fluorescence microscopy of

the fully hydrated bacteria in water: large colonies grew on the flat polystyrene, while no large colonies were observed on the samples coated in spheres.

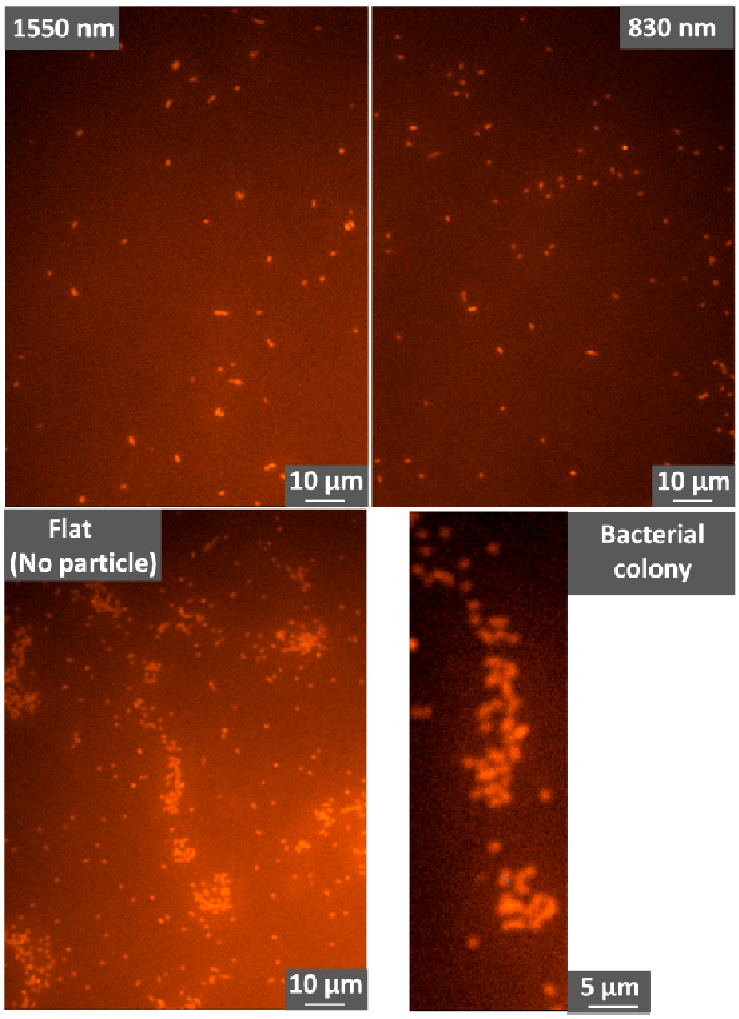

Fig. 3- 2. Fluorescence images showing *P. aeruginosa* on polystyrene colloidal crystals (1550 nm and 830 nm diameter spheres) and on a flat polystyrene sheet.

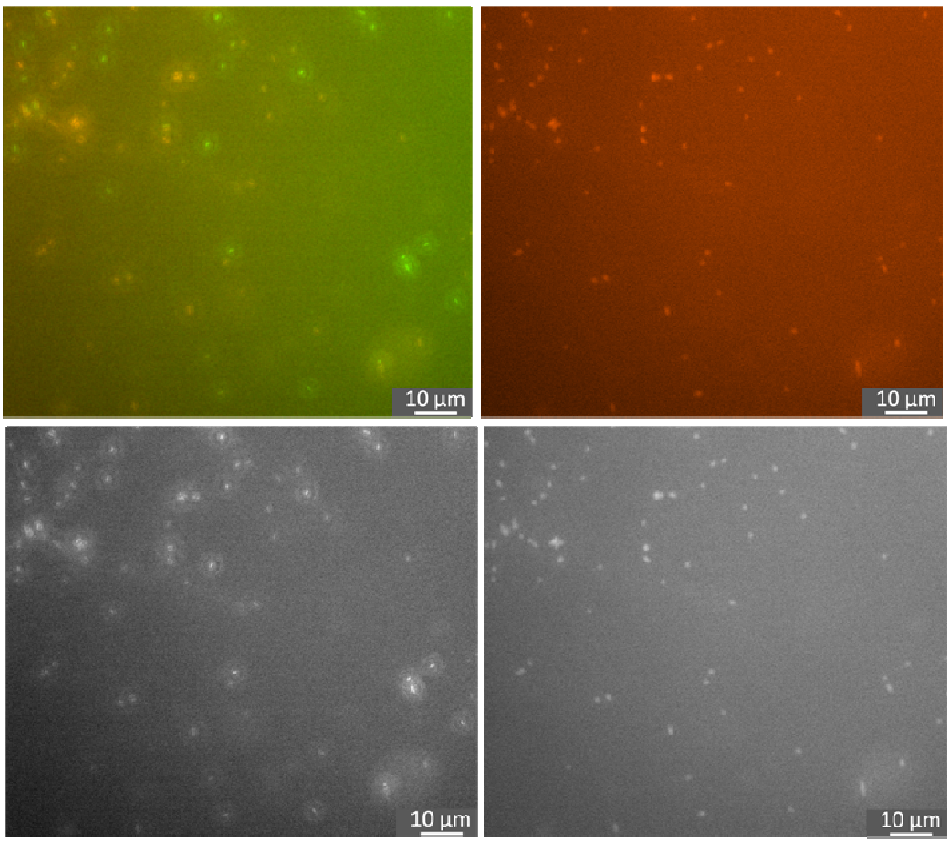

Fig. 3-3. Fluorescence image of bacteria adsorbed to 1550 nm colloidal crystal. Left: In water. Right: after exchange of the water for ethanol then air drying for 3 hours. The original fluorescent images are on the top row and processed images are shown in the bottom row. Note that the position of each bacterium remains unchanged after each stage of preparation that is used for the SEM samples.

To enable higher resolution imaging of colloidal crystals and the bacteria, we also performed SEM imaging. Sample preparation for SEM requires dehydration and drying of the bacteria, so we first tested whether our SEM sample preparation altered the distribution or number of cells on the solid. Previous work has shown that the passage of *air bubbles* in water can alter surface distributions of bacteria.[54] As shown in figure 3-3 exchange of the solution with ethanol, then air-drying affected neither the number density, nor the arrangement of the *P. aeruginosa* on the colloidal crystal and flat

surfaces. Likewise figure 3-4 shows that the passage of the ethanol-air interface across a particle does not change the position of the bacterium.

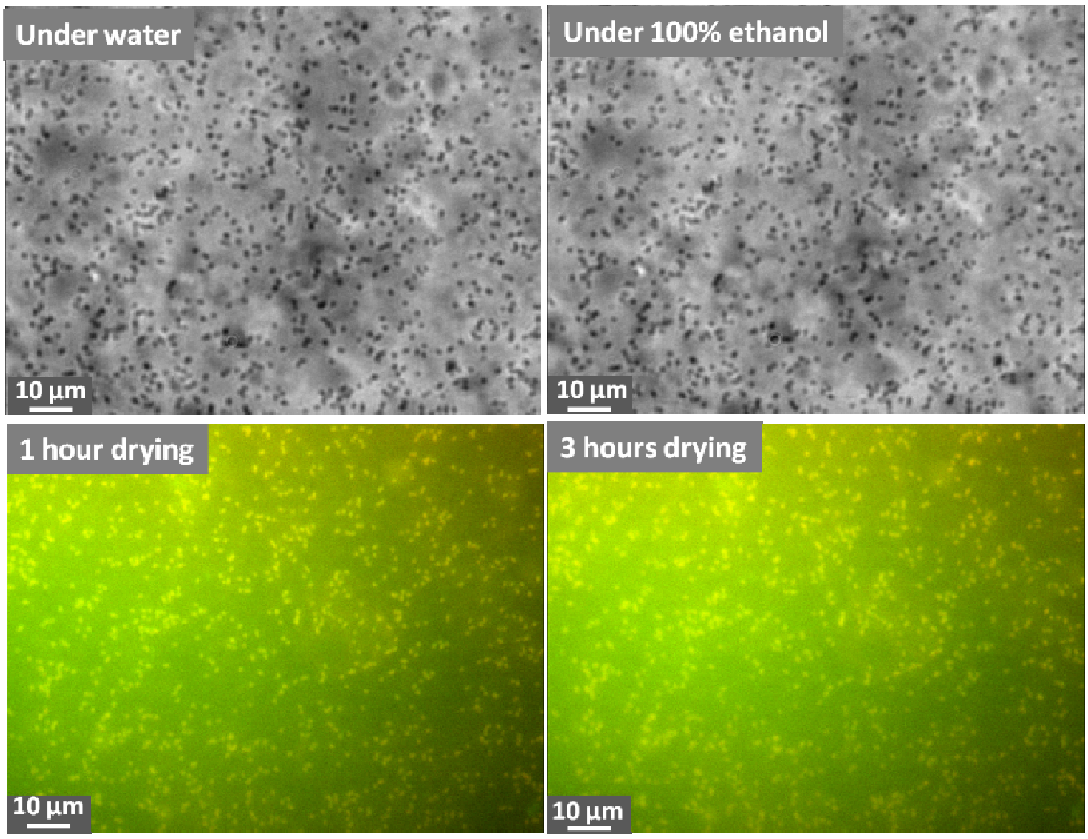

Fig 3-4. Sequence of fluorescence images of *P. aeruginosa* (PAO1) bacteria adsorbed to a flat sheet. The arrangement of bacteria in this image is not typical for *P. aeruginosa* on a flat polystyrene sheet. In a typical image of a flat surface, the bacteria are arranged in colonies as shown in Figure 3-2. This unusual area is shown so that one can examine whether the process of drying that is used prior to SEM imaging gives an artifact that looks like colony formation on a flat sheet. The sequence is: under water, then after replacement of the water with ethanol, then 1 hour of drying then 3 hours of drying. Note that the position of each bacterium remains unchanged after each stage of preparation that is used for the SEM samples: drying does not produce an artifact that looks like colony formation.

Knowing that the sample preparation does not affect the distribution of bacteria, we can use SEM to examine the effect of the colloidal crystal in more detail. The SEM image in figure 3-5 shows large colonies on flat surfaces, with the same distribution as in the optical images.

Our first objective is to examine how the spheres affect micro-colony formation. A colony is a collection of cells in which there is close contact,[55] but there is no universal definition of the number of cells required for a colony. For the purpose of quantification here, we will define a colony as a collection of bacteria which has more than 10 cells. Table 3.3 shows three quantities for both flat and colloidal crystals: 1-Colony density: The number of colonies per 1 mm^2 of the projected area of a sample, 2-Colony size: The average number of cells in a colony, and 3-% in colony: The number of bacteria in colonies divided by the total number of cells available on the surfaces.

Table 3-3. Colonization parameters for flat and colloidal crystals.

Diameter	**flat**	**220nm**	**450nm**	**630-1550nm**
Colony density (colony/mm^2)	732	446	38	0
Colony size (cells/colony)	56	20	12	0
% in Colony	83	22	5	0

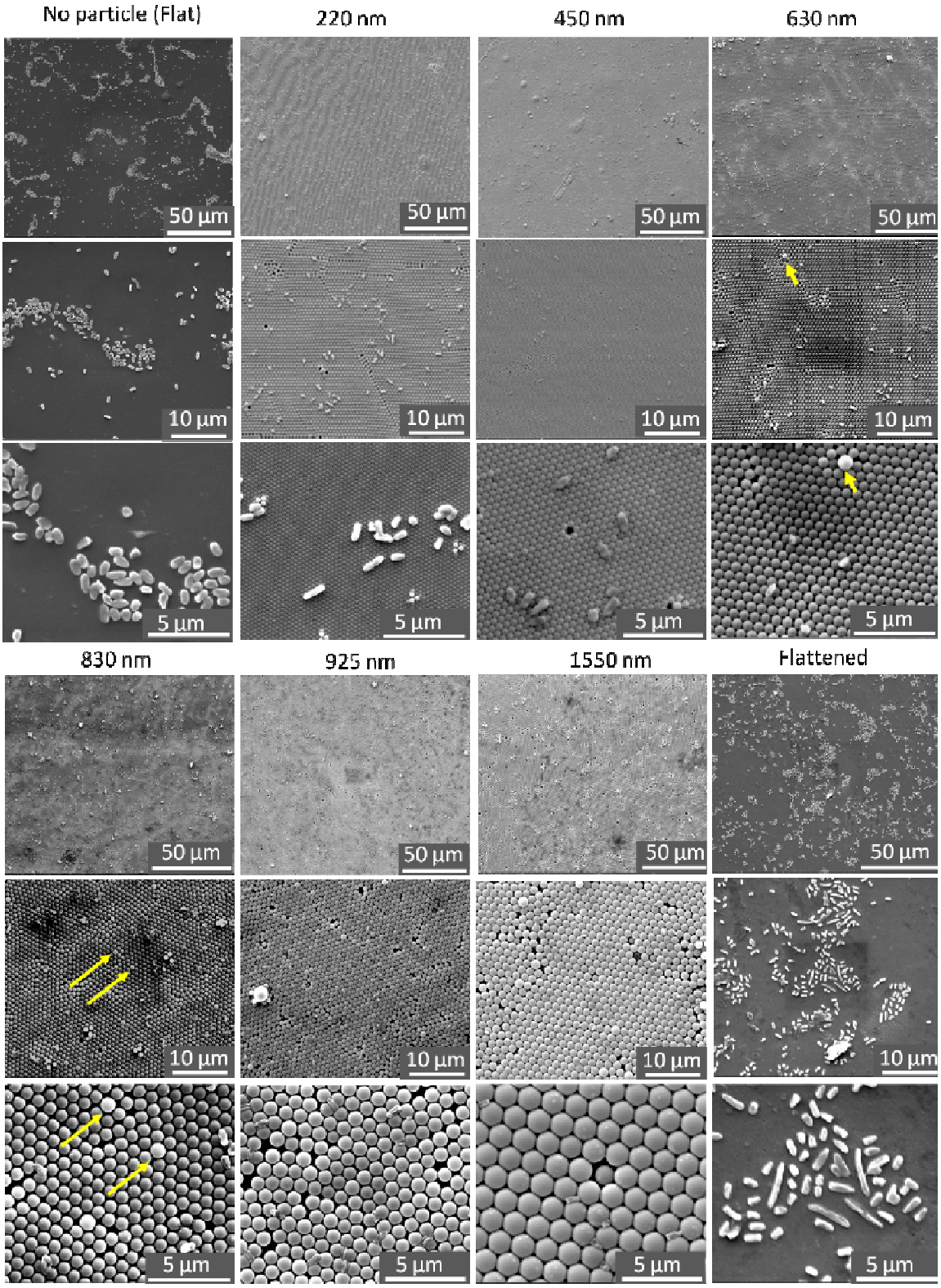
No particle (Flat)
220 nm
450 nm
630 nm
50 µm
10 µm
5 µm
830 nm
925 nm
1550 nm
Flattened

Fig. 3-5. SEM images of *P. aeruginosa* on polystyrene samples with and without a monolayer of colloidal crystals. The last column shows large *P. aeruginosa* colonies on flattened polystyrene samples (fabricated from 450 nm particles and then annealed.) The numbers above each column of 3 images show the diameter of the polystyrene particles that were used to form the colloidal crystals. Note that bacteria and spherical particle sizes are similar in some cases, making it difficult to distinguish bacteria from defects such as large particles in the 50 μm images. The arrows (630 nm and 830 nm samples) point to larger than average particles that are easy to distinguish from bacteria in the higher magnification images.

Our results indicate that adding smaller particles (220 nm) to the surface will reduce both size of the colony and the density of the colonies. An even smaller density of even smaller colonies was observed on the 450 nm colloidal crystals; only 5% were involved in colonies. The average colony size was only 12 and if we had made our arbitrary definition of colony to be 16 cells, then there would be zero colonies on the 450 nm sample. *No colonies were observed on crystals formed from the larger spheres.* Thus all the sphere sizes reduced the number of colonies.

Experiments using *flattened* samples typically produced similar results as those on the flat polystyrene shown in figure 3-5, i.e. large colonies formed. Thus, comparing the colloidal crystal samples to the *flattened* samples (which were formed from exactly the same material) we conclude that the topography prevented colony formation on the colloidal crystals. Comparing the *flattened* samples to the flat sheet samples, both allowed the formation of colonies, thus variation in zeta potential of the polystyrene under the FBS-deposited layer was not the determining factor for colony formation in this

work.

3-3-2-B. Reducing the number of bacteria.

Although the presence or absence of colonies is clear from the optical and SEM images, the area density of bacteria provides a quantitative comparison of the effect of the colloidal crystal. The data in figure 3-6 shows the relative density of bacteria adhered to each colloidal crystal as a function of particle diameter (d), defined as:

$$\text{Relative Density } (d) = \frac{\text{number on colloidal crystal-coated surface}}{\text{number on flat surface}} \qquad (3\text{-}1)$$

where "number" refers to the number of bacteria per unit area, and for numerator, the area refers to the area of the polystyrene sheet under the colloidal crystal. Although there was variability in results on each experiment (the standard deviation for all data on the flat surface was 50% of the average), normalization by the result for a flat sheet in the same experiment removes the effect of this variability. Each datum for the same diameter represents the average value from samples observed in independent experiments (i.e. a different set of samples on a different date in the same reactor).

We conducted a one way analysis of variance (ANOVA) followed by a Tukey test to determine whether there was a significant difference ($p \leq 0.05$) between the relative densities of bacterial colonies at different particle diameters. The ANOVA test showed that the relative density of bacteria adhered to the 220 nm particle film was not significantly different from the density on the flat surface. The diameter did not have a significant effect on the relative densities of bacterial colonies for the particle size range 450–1550 nm. However, we did observe a significant difference between the number of bacteria per unit area on the flat surface and any sample using spheres in the size range

450–1550 mn: the number of bacteria was reduced by more than 80% on these larger-diameter colloidal crystals.

In summary, the 450–1550 nm particles prevented the formation of large colonies and reduced the number of bacteria by about 80% compared to the flat surface. The 250 nm particles did not reduce the number of bacteria, but still inhibited the formation of large colonies.

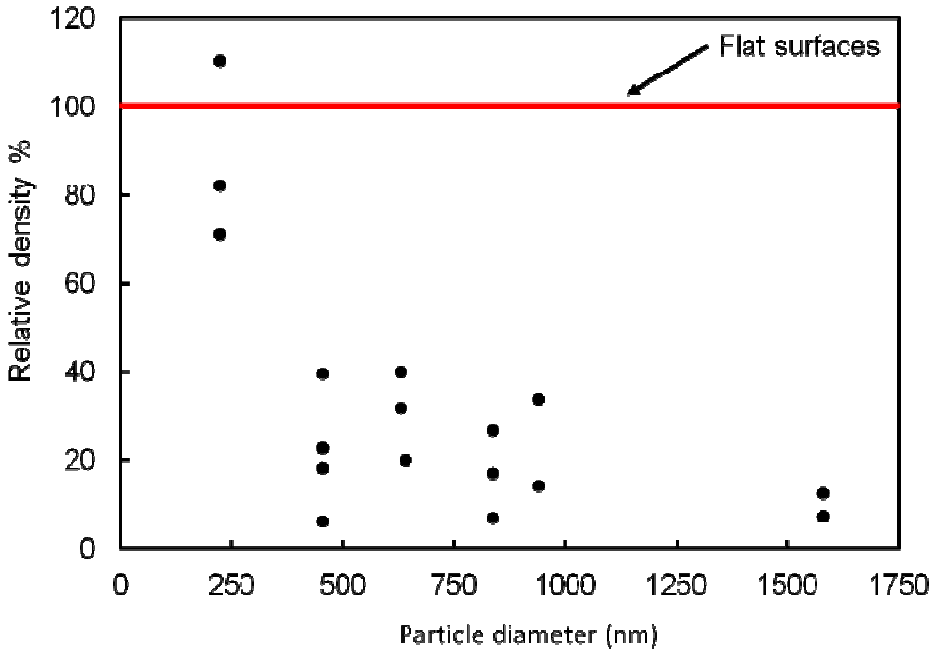

Fig. 3-6. Effect of particle diameter on the relative density of *P. aeruginosa* bacteria adhered to close packed colloidal crystals of polystyrene spheres. A relative density of 1 is defined by the number per unit area on a flat polystyrene sample. The number density of the cells adhered to flat surface is 50000 cells/mm^2 with a standard deviation of 24000 cells/mm^2.

3-3-2-C. The Distribution of bacteria among differing sites on the colloidal crystal

The colloidal crystal provided the bacteria with a variety of binding sites that are shown schematically in figure 3-7: the crown, the 3-fold site and the 2-fold site. P.

aeruginosa is approximately cylindrical in shape with variable size, but typically has a long axis of about 1300 nm and a short axis of about 500 nm (see SEM images). We selected a range of particle diameters ranging from smaller than the bacterial dimensions to larger, such that a bacterium must straddle several sites on the 220 nm particles, whereas all *P. aeruginosa* dimensions are smaller than the 1550 nm particles. The images in figure 3-5 show that selectivity among sites depends on the diameter of the particles: for the 220 nm particles, adhered bacteria spanned many sites; for the 630 nm and larger particles, the bacteria showed a preference for positioning the body in a 2-fold site: 100% were in this site. In the Discussion we hypothesize that the mechanisms of this selectivity are related to the costs associated deformation of the bacteria, the number of contacts, and the arrangement of favorable adhesion sites.

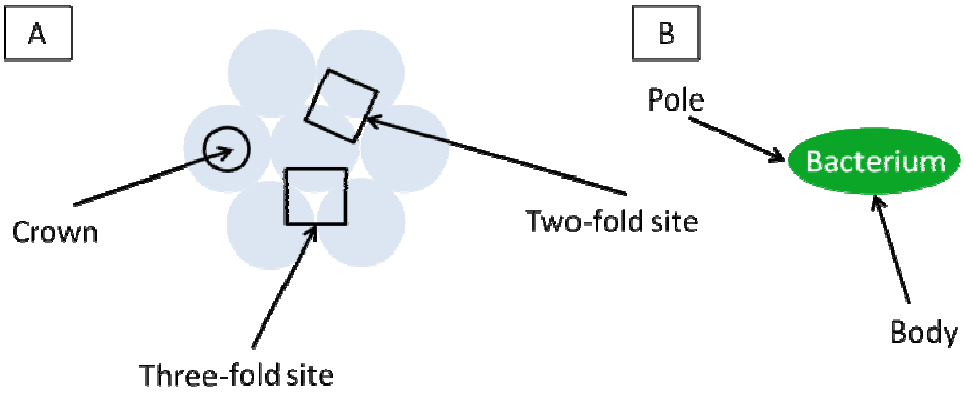

Fig. 3-7. A) Schematic of the colloidal crystal showing the sites discussed in the text. B) Nomenclature used to describe bacteria.

3-3-2-D. Application to medically-relevant materials.

One of the major advantages of using colloidal crystals for inhibiting microbial colonization is the ability of the method to be applied to surfaces with complex geometries and chemistries[23-25]. Here we examine briefly a stainless steel needle, which

is a different material with a different geometry, to see whether a colloidal crystal film reduces the incidence of colony formation.

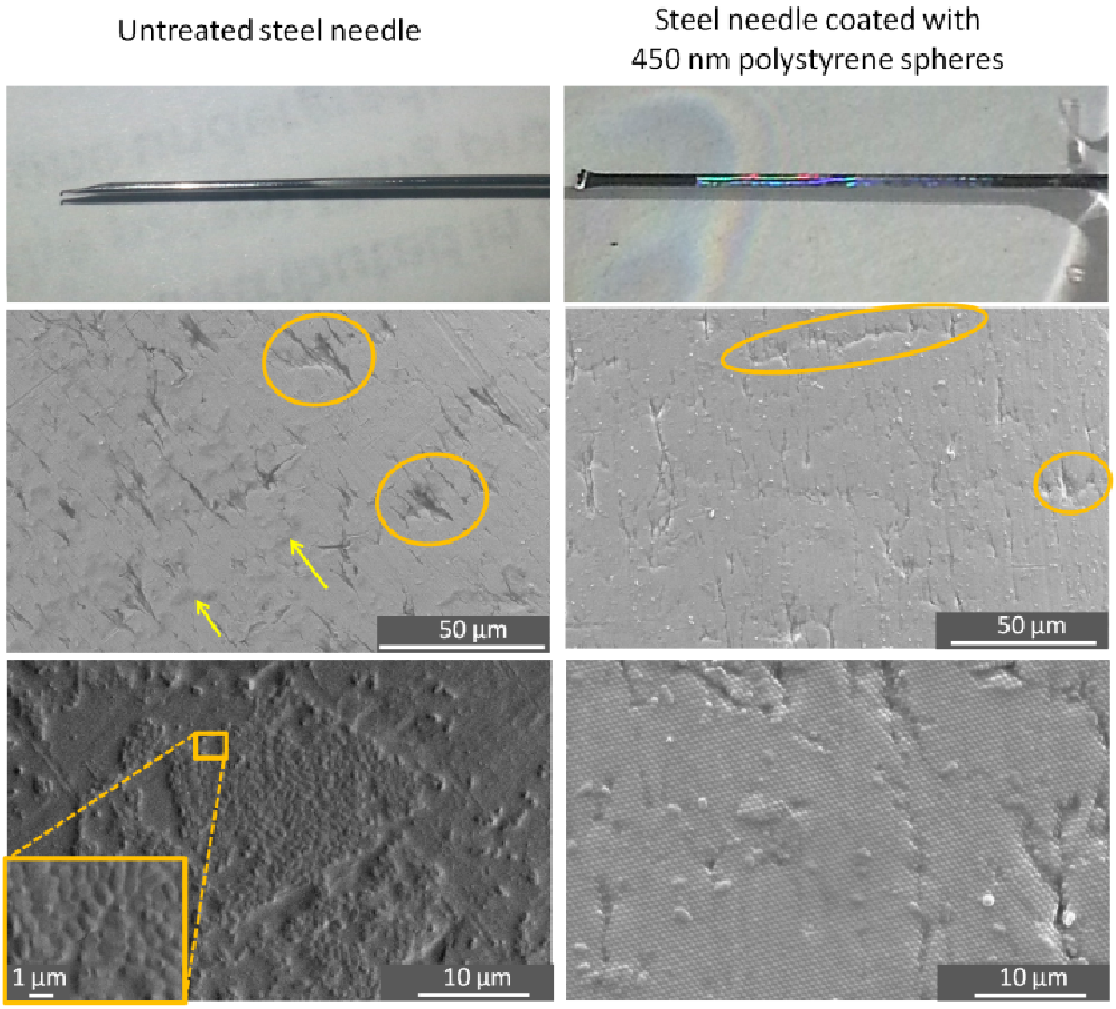

Fig. 3-8. Effect of 450 nm pack polystyrene spheres on microbial colonization of a biomedical grade steel needle (diameter = 1.5 mm). The needle has a rough, scratched surface. Example scratches are highlighted with ovals in the images. The top row shows the photograph of a untreated steel needle (left) and the steel needle treated with 450 nm close-packed polystyrene spheres (right). The middle row shows low magnification SEM images of the surfaces of untreated (left) and colloidal crystal- treaded surfaces (right) after exposure to the *P. aerugniosa* in a CDC reactor for one day. Arrows on the left figure point to microbial colonies on the

untreated stele needle. Bottom row: Higher magnification SEM images of the images showing large microbial colonies on untreated surface of steel needle (left) and the absence of colonies on the colloidal crystal treated surface (right).

A colloidal crystal coating was prepared on the needle using the same method as for the flat polystyrene substrate. The optical photograph showing an opalescent film on the needle in figure 3-8 signifies that a colloidal crystal (450 nm particles) can be deposited on a curved material that is not polystyrene, and SEM imaging shows that the particles are arranged in much the same way as on a flat sheet of polystyrene. The SEM pictures in figure 3-8 demonstrate that colony formation is dramatically hindered on the colloidal-crystal-coated needle compared to the untreated needle.

3-4. Discussion

3-4-1. Concepts of selective adhesion

The SEM images show that the bacteria are not randomly distributed across the samples: specific locations have a greater density of occupation. Previous work suggests that both strain specificity and motility are important factors in selectivity.[11, 22, 29, 30, 14, 18, 21, 24-26] With respect to motility, Scardino *et al.*[24] compared the interactions of motile and non-motile marine organisms with topographically engineered surfaces and reported that whereas the number of adhered motile cells depended on the topography, the number of adhered non-motile cells did not. Kargar *et al.*[21] observed similar behavior for *P. aeruginosa* PAO1: wild type *P. aeruginosa* selectively attached to specific binding sites on fibrous surfaces whereas the non-motile pila mutants, (lacking type IV pili, used for surface motility) lacked selectivity. Furthermore, *P. aeruginosa*, has been observed to show selectivity in its alignment relative to topographical features.[15, 17, 27]

The preference for particular sites on the colloidal crystal observed in this work suggests that *P. aeruginosa* does discriminate among different sites. This discrimination should have two aspects: (1) the ability to move between two sites and (2) differences between sites that affect the occupancy of the site by the bacterium. The ability to move between sites can be provided by the motile elements such as pili or flagella, or by passive action such as diffusion or fluid flow (provided by stirring in our experiments).

Given the opportunity to explore, the second component of selective adhesion is discrimination among different sites. Bacteria are complex: they have proteinaceous features in their membrane which contribute in their adhesion to the surfaces, secrete polymers to enhance adhesion[56], and they can communicate[57]. All these factors may be important, but here we focus on the physical properties of deformation and adhesion and the relationship to topography. Kargar *et al.*[22] explained selective adhesion of *P. aeruginosa* to fiber-coated surfaces based on a balance between adhesion energy and deformation energy, following the work on vesicle adhesion described by Seifert and Lipowsky.[37] In the same vein, we make an assumption: a favorable adsorption site is where a large area of contact can be achieved between the bacterium and the solid. The logic behind the assumption is that a large area enables a strong adhesion if adhesion is proportional to the area of contact. At each point where a bacterium contacts a solid, the bacterium may deform or secrete compounds to increase the contact area, but each of these costs energy. The important aspect of our colloidal crystals is the bacterium can only contact a sphere, and, each sphere curves *away* from the bacterium, meaning that, as the area of the contact grows, the distance of deformation grows, and so too does the cost. The smaller the radius of curvature of the contact point on the sample, the greater the

deformation or secretion required to increase the contact area.

A sphere has the same curvature at every point, so there is no advantage to adsorbing on a particular point of the sphere. However, in addition to adhering to a single contact, a bacterium can increase the total area of contact by finding a second sphere to contact. (Providing a new contact is in range, growing a new contact requires less energy than extending an existing contact because less deformation is required.) Selectivity on a uniform packed layer of spheres must arise from differences in the *number* of contacts that are available to a bacterium. Thus, following our assumption, a favorable position is one where the bacterium can contact several spheres, and thus where the spheres are closer together than a dimension of the bacteria. The 2-fold and 3-fold sites provide such a location whereas the crown is further away from other spheres and should be less favorable.

We now discuss these concepts of selective adsorption in relation to the experimental results. For diameters greater than 450 nm, there were no bacteria adsorbed to the crown (see figure 3-5): using the concepts above, this is because crown is the point where it is the maximum distance to another sphere for forming a second contact. On spheres in the diameter range 630–925 nm, a single bacterium is more likely to be straddling two 3-fold sites: this is because the bacterium can contact four spheres in this position. For the 230 nm particles, the discrete nature of adhesion sites is smeared out because the length and width of each bacterium is greater than the diameter of the particles: each bacterium can bind to several spheres regardless of where it sits on the surface. Because all positions on the 230 nm surface are now similar, the arrangement of the bacteria is less influenced by the topography.

It is also possible that variation in shear rate plays a role in selective occupancy of different positions. The crown projects further into the flow field than the more sheltered sites between the spheres and therefore is likely subjected to greater shear stresses that could remove bacteria.

3-4-2. Reduced density of bacteria on colloidal crystal vs flat plate

The flat plate does not curve away from the bacterium, so less deformation is required to increase the contact area. Thus the flat plate is immediately more favorable for adhesion if the only consideration is the deformation required to achieve a suitable contact area.

3-4-3. Trends in relative density of bacteria

As the radius of the particles increases, we believe that the following factors may be important: (1) less deformation is required for the same contact area on a single sphere; (2) there is an increase in the spacing between centers of the spheres, which causes a lower density of (favorable) 2-fold and 3-fold sites, (3) changes in compatibility between bacterial dimensions and binding dimensions (epitaxy) and (4) the binding sites become deeper, leading to better shelter from shear forces. The near constancy of the relative adhesion with diameter in the range 450-1550 suggests that exact matches in dimensions are not resolved or not important for the adhesion of *P. aeruginosa* . The first factor is expected to cause an increase in adhesion density with increasing radius whereas the second factor (diminishing density of 2-fold and 3-fold sites) should lead to an overall decrease in density of bacteria. This can also be considered as an increase in the area covered by the unfavorable crown area. The combination of opposite trends may be responsible for the fact that we observed approximately constant adhesion density as a

function of diameter (Figure 3-6).

For 230 nm spheres, the relative density of adhesion is about the same as on the flat substrate, and significantly greater than on the larger spheres. The local curvature of each spherical particle is greater on the 230 nm particles, which means that greater deformation is required for the same area of contact at each contact - an unfavorable factor. However, the large size of *P. aeruginosa* (~500 nm × ~1300 nm) compared to the sphere diameter enables the bacterium to make contact with multiple particles (e.g. 10-20) and therefore the total bacterium–sphere area can be still high enough to favor adhesion.

3-4-4. Formation of colonies

In our experiments there is a correlation between selective adhesion and inhibition of colony formation. There are two possibilities that might explain this correlation. First, the locations where single bacteria are observed (2-fold or 3-fold sites) may not be conducive for biological phenomena such as reproduction or recruitment, which may inhibit colony formation. Future tests would be required to examine this possibility.

Second, colony formation may be inhibited because the lack of *adjacent* favorable sites. The essence of a colony is close proximity (usually contact) of bacteria. But if there are no adjacent favorable sites, then some bacteria in such a colony must sit on an unfavorable site. Occupation of such a site may be so unfavorable that bacteria do not reside there and thus colonies cannot form. Referring to our colloidal crystals, for particle diameters larger than 450 nm, the individual bacteria prefer to site in the 2-fold

and 3-fold sites and are not found on the crowns. To cover the entire surface would require some bacteria to sit on the less-favorable sites, and that may simply be too unattractive. Thus, one hypothesis for the lack of colony formation on particles greater than 230 nm is that adjacent favorable sites are simply too far apart.

3-5. Conclusions

We compared interactions of *P. aeruginosa* with both flat surfaces of polystyrene and surfaces coated with a monolayer of close-packed spheres. The colloidal crystal-coating reduces the number density of *P. aeruginosa* adhered to the surface, reduces the number of microbial colonies, and alters the arrangement of the cells. In particular: (1) the colloidal crystal reduced the number density of bacteria adhered to the surface by about 80% for particle diameters in the range 450–1550 nm; (2) spheres with diameters in the range 220–1550 nm reduced the incidence of colony formation, and no colonies were observed when the particle diameter was in the range 630–1550 nm and (3) for particle diameters exceeding 630 nm, *P. aeruginosa* selectively adhere in the 2-fold sites and are rarely found on the particle crown. Our results are consistent with the idea that it is more difficult for bacteria to adsorb to curved surfaces, and that bacteria select between different surface sites based on the local geometry. Furthermore, the results are consistent with the idea that the formation of colonies can be influenced by the proximity of favorable adsorption sites for individual bacteria.

The incidence of bacterial colony formation on a medical grade stainless steel needle (diameter = 1.5 mm) was reduced by coating it with 450 nm particles. This result suggests that application of a layer of colloidal particles is a promising strategy to delay

adhesion and colony formation of microbes on a variety of materials and geometries.

Chapter 4. Colloidal Crystals Delays Formation of Bacterial Biofilms

Abstract

We[3] investigated the cluster formation, micro-colony growth, and 3D biofilm formation of *Pseudomonas aeruginosa* PAO1 on a solid coated in close-packed spheres of polystyrene (a colloidal crystal). The objective was to determine whether formation of biofilms would be delayed on curved structures compared to flat surfaces. The curvature was of the order of the bacterial dimensions. Solids were pretreated with serum and then exposed to bacteria under low shear for two days in a center for disease control biofilm reactor. During the second day the reactor was fed with nutrients in order to support the biofilm growth. After two days, 3D biofilm structures cover much of the flat polystyrene, whereas 3D biofilms rarely occur on a solid with a colloidal crystal coating of 1550 nm spheres. On 450 nm colloidal crystals, the bacterial growth was intermediate between the flat and 1550 nm samples. These biofilms are similar to early stage of typical mushroom-shape biofilms formed by *P. aeruginosa*. In addition to hindering biofilm formation, the colloidal crystals also affect the organization of bacterial clusters. The cells on the 1550 nm particles have a preference to sit in the gaps between the particles and to have a preferred orientation parallel to the axes of the crystals. Although the cells form clusters, the body of the cells rarely touch in the cluster, and when the cells do touch, the contact is usually the pole, not the sides of the bacteria. We concluded that the anti-biofilm property of the colloidal crystals is correlated with the ability to arrange the individual cells. This arrangement is discussed in the context of the potential gain

[3] This chapter will be submitted as a journal paper. The authors are Mehdi Kargar, Hamoun Khalili Hoseinabad, Amy Pruden and William A. Ducker

and costs that contact of the cells with crown, confined space or to each other may have.

4-1. Introduction

Adhesion of microorganisms to surfaces can lead into formation of microbial communities known as biofilms. From a medical perspective, a biofilm is troubling organization of microorganisms because it is responsive to both the host immune system, and to treatments by antibiotics.[2] Compared to planktonic (free floating) cells, the cells in a biofilm can have altered gene expression and metabolism, and be specialized within the biofilm.[58] Figure 1-1 is a schematic of the steps involved in biofilm formation: macromolecules adsorb to an interface, then planktonic cells adsorb. Under favorable conditions the adhesion may become stronger and irreversible. Irreversible adhesion can lead to formation of small clusters of cells, either by reproduction, or by addition of cells from the aqueous phase or by surface migration. Under favorable conditions, the small clusters can grow into colonies, and finally evolve into 3D biofilm structures. The objective of the current work is try to delay or interrupt the progression to a biofilm by modifying a solid surface. In particular we investigate the use of adsorbed particles to modify the surface topography.

Prior work has shown that topographical modification of surfaces can affect subsequent interactions with bacteria[13, 15-19, 21-23, 30, 50-52] and other microorganisms.[7, 11, 14, 24-26] For example, Chung et. al[15] showed that patterns of approximately rectangular ridges (Sharklet™ surfaces) in polydimethylsiloxane (PDMS) delayed biofilm formation by *Staphylococcus aureus*. The proposed mechanism was that "the protruded features of the topographical surface provided a physical obstacle to deter the expansion of small clusters of bacteria present in the recesses into microcolonies."[15] The Sharklet surface was also show to reduce the number of adsorbed *Mycobacterium abscessus*.[59] Likewise,

Xu and Siedlecki[30] observed that biofilm formation by *S. aureus* or *Staphylococcus epidermidis* was delayed on pillars of poly(urethane urea) compared to flat surfaces. They attributed their observation to the potential effects of the hydrodynamic shear forces present in their experiments. Xu and Siedlecki,[30] hypothesized that if texturizing the surfaces reduces the available contact area between the cells and the solid surface, it can support ease of cell removal and delay biofilm formation. Ivanova et al[60] have explored a different use of topography: to penetrate and kill bacteria. They showed that the sharp spikes on cicada wings could kill *Pseudomonas aeruginosa* cells.

Our hypothesis is that coating surfaces with assembly of microspheres can delay biofilm formation. We based this hypothesis on the potential effects of the local curvature on the microbial adhesion to the surfaces described by Kargar et. al.[22] They hypothesized that engineering the local curvature of surfaces will result in reduction in the number of cells adhered to a solid, and gave results for the number of *P. aeruginosa* as a function of the radius of adsorbed fibres. The proposed mechanism was that adhesion to the curved surfaces can require greater deformation of the cell body and consequently greater energetic cost for the cells in order to attach. This idea was based on theories of the adhesion of vesicles[37] to the surfaces.

In our previous publication,[50] we investigated the effect of colloidal crystals on adhesion and early stage cluster formation by *P. aeruginosa*. *P. aeruginosa* is a gram-negative, motile, rod-shaped bacteria that acts as opportunistic pathogen.[32] A colloidal crystals is a regular array of particles. In particular, we investigated hexagonally-packed microspheres because spheres have controlled curvature at every point. Figure 4-1 shows a schematic of the colloidal crystals. In that work, we showed that coating surfaces with

colloidal crystals reduces the number of *P. aeruginosa* adhering to the surface after one day, and the number of bacterial clusters, and causes selective adhesion to the two-fold sites in the crystal. In this paper, we extend that study to longer times to investigate how colloidal crystals affect the progression to a biofilm, which is the important structure in medical infections.[58] Our goals are to minimize biofilm formation, and to understand the mechanisms by which this might be achieved.

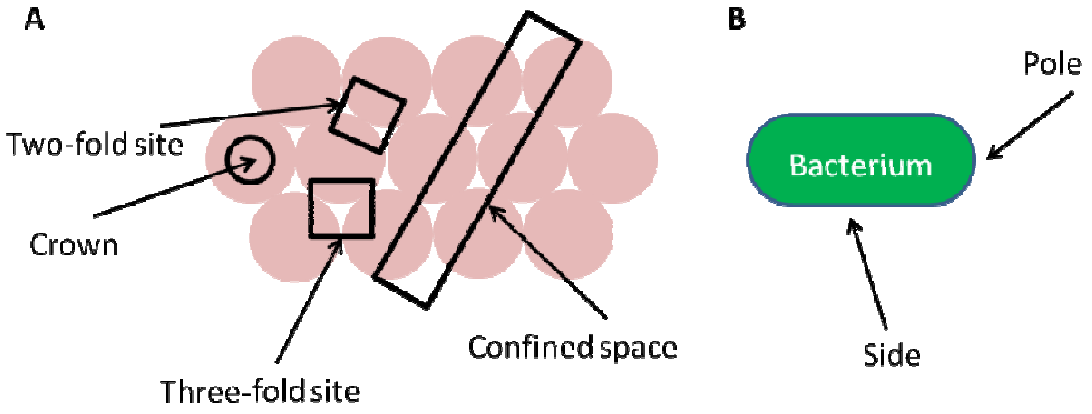

Fig 4-1. A) A Schematic of the colloidal crystal geometry. We refer to the groove shape gaps between the particles as “confined space”. B) Schematic of bacteria clarifying the terms "side" and "pole" of bacteria as used in this paper.

Although, the bioflm formation of *P. aeruginosa* on flat surfaces has been widely studied in pastt, [31, 33, 34] but studies on interaction of *P. aeruginosa* with topographically engineered surfaces were mainly focused on adhesion and early stage colony formation.[17, 18, 21, 22, 50] Therefore, our results here also provides new insights on the effect of the surface topography on biofilm formation by *P. aeruginosa*.

4-2. Experimental

4-2-1. Flow-through biofilm formation assay

The samples were cleaned and sterilized as described previously[50] and then incubated under FBS overnight to mimic the adsorption of a conditioning film that occurs in a natural environment. The samples were placed in a Center for Desease Control (CDC) biofilm reactor (BioSurface Technologies Co., Bozeman, MO), the reactor was filled with 363 ml of 100 times diluted TSB, ie. 300 mg/L TSB) and then 1.7 ml of bacterial culture ($OD_{600} \approx 0.06$) was added. During the first day, there was no nutrient flow to the reactor, and bacteria adhered to the surfaces and grew using nutrient available inside reactor. During the second day, the bacteria were fed by pumping the nutrient (300 times diluted TSB, ie. 100 mg/L TSB) at a constant flow rate for 24 hours. The flow-through system consisted of a nutrient carboy, a peristaltic pump, and a waste carboy connected by silicone tubing, as described by Goeres et.[48] and is shown in Fig. 4-2.

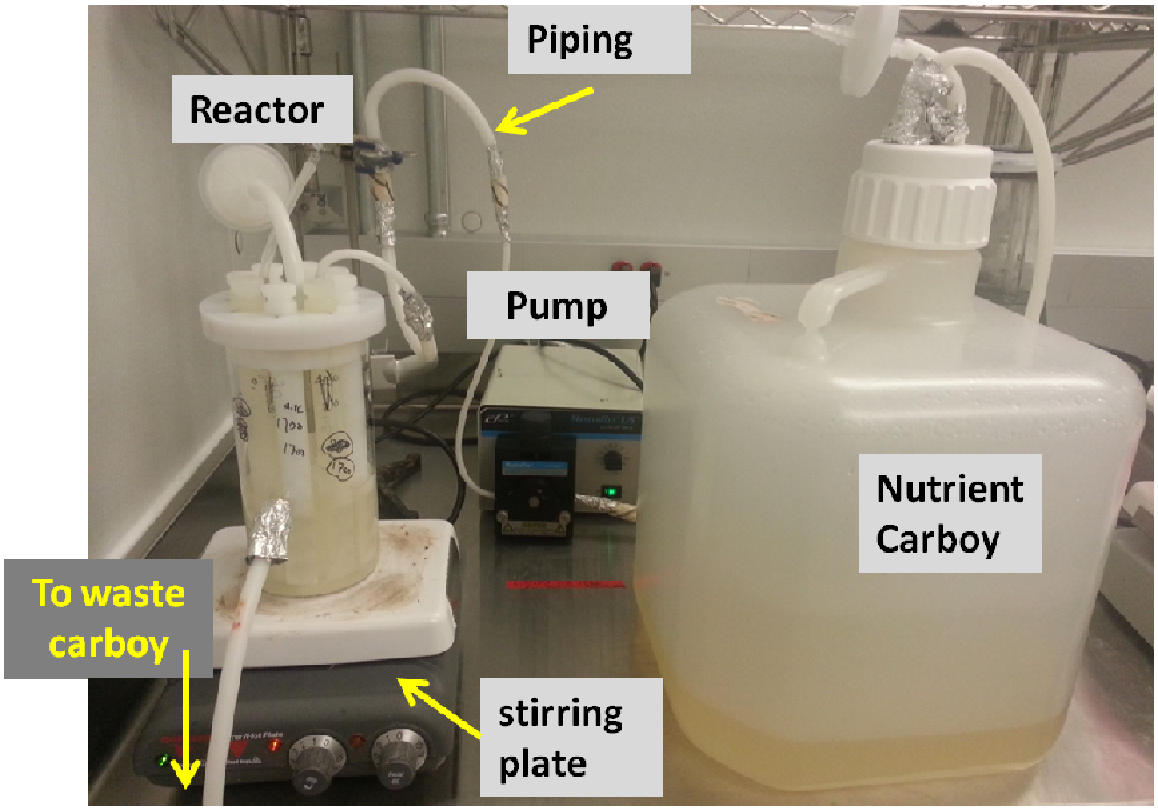

Fig. 4-2. A photograph of the flow through system used to grow biofilm on surfaces inside the reactor. The pump supplies nutrient from nutrient carboy to the reactor throughout the piping. The waste flows gravitationally to the waste carboy (not shown here). Stirring plate controls the rotational speed of the baffle stirred inside the reactor. Figure 2-2 provides further details about the reactor.

Our model microorganism was *P. aeriginosa* (ATCC^{R} 47085^{TM}). During the first day the solution inside the reactor became cloudy through growth of bacteria, but after the second day, the reactor media was transparent due to flux of fluid through the reactor. Experiments were conducted in a controlled temperature room at 37℃ with stirring at 50 RPM. [50] t the end of the two days, the samples were washed once with DI water, and then fixed in 2.5% glutaraldehyde, so all analysis was done on dead bacteria that were in a fixed state.

4-2-2. Confocal laser scanning microscopy (CLSM)

Samples were attached to the bottom of a glass-bottom Petri dish, stained with the live-dead stain and imaged while hydrated and submerged under the dye solution using confocal microscopy. The microscope consisted of a Zeiss LSM 510 laser scanning microscope, Axio Observer Z1, 40x water immersion objective, and ZEN 2009 software. Further detail for sample preparation can be find in section 2.7.

4-2-3. Image processing and data analysis

Figure 4-3 shows the image processing steps conducted to quantify the effect of colloidal crystals on formation of biofilm structures.

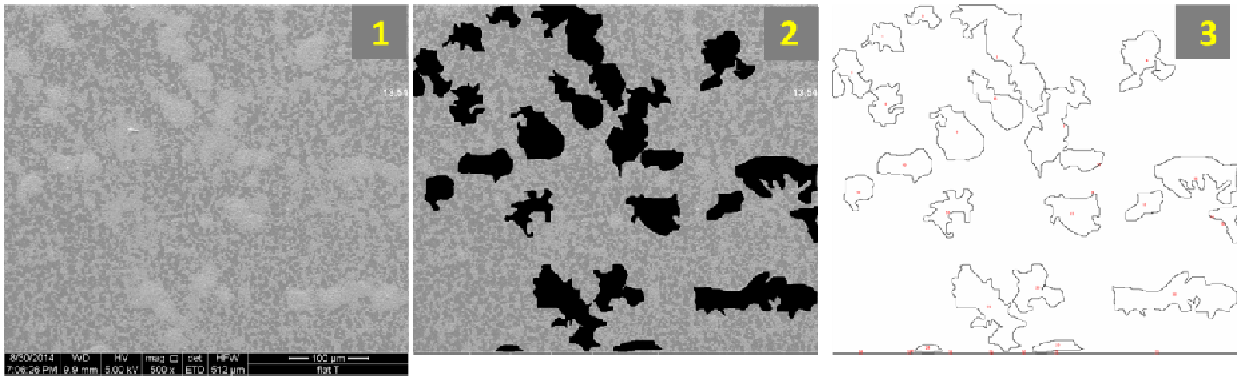

Fig. 4-3. Image processing steps conducted to quantitatively analyse the fraction of a sample covered in a biofilm, and the area of each biofilm. Step 1. SEM images of bacteria on sample (magnification: 500X). Step 2. The area covered with 3D structures was determined by visual inspection and manually masked (black structures). Step 3. The total number and size of each biofilm within the masked areas was calculated using ImageJ. Images for analysis were determined from a grid of 16 points on a low magnification image (e.g. 20–40×) of each sample (1.5×0.5 mm^2). The images for analysis were at 500× magnification. The areas close to the edges were not used for analysis.

4-3. Results

4-3-1. Effect of colloidal crystals on biofilm formation

4-3-1-A. Delaying formation of biofilm

Our primary objective was to determine whether a layer of colloidal crystals either slowed or prevented the biofilm formation over a period of two days during which the solution conditions encourage the growth of bacteria. Here we identify biofilms via their growth into dense 3D structures, that is, structures where there is more than one layer of bacteria (See schematic on Fig. 1-1). Solid samples were initially immersed in medium (324ml of 300mg/l TSB) inoculated with bacteria, and then, after 24 hours the reactor was continuously fed by fresh nutrient (100mg/l TSB at 10.5 ml/min). Experiments were repeated three times, and typical images of the bacteria on the 450 nm particles, 1550 nm particles, and the flat (control) after two days of exposure are shown in Fig. 4-4. The left column shows confocal images that were captured from fully hydrated samples. The red stain stains the bacteria so the bright red areas show high densities of bacteria, which indicates a biofilm. Clearly, there are many more bright patches on the flat substrate than on the colloidal crystal: there is only one such structure on the 450 nm sample and there are none on the 1550 nm colloidal crystal. An analysis of cross-sections of the images shows that on the flat substrate, the bright areas are about 8 μm high and on the 450 nm colloidal crystal the bright structure is only about 5 μm high, whereas the cells are rarely more than one layer thick on the 1550 nm colloidal crystals. So, we conclude that that are more biofilms on the flat sample than on the colloidal crystal, and that they are more developed. There is no biofilm on the 1550 nm spheres. Thus the colloidal crystals

delay the formation of biofilm.

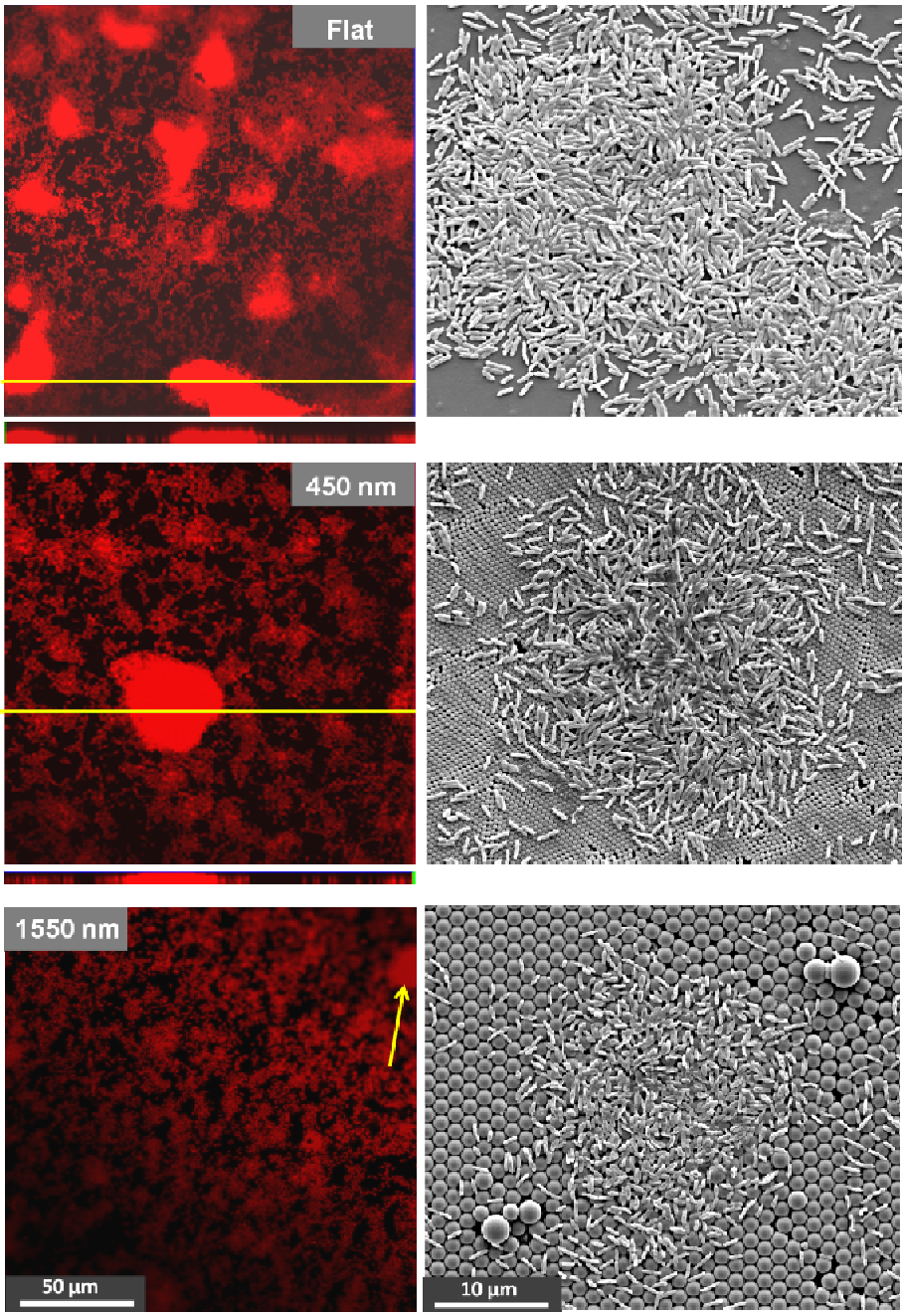

Fig. 4-4. Left column: confocal images of P. aeruginosa, PAO1, adhering to solid samples under dye solution after two days. Because the cells have been fixed they show as dead in the live-dead stain. Cross-sections through the bright areas (shown below the images of the flat and 450 nm samples) show that the bright areas are 3D structures formed by bacteria. The vertical scale is the

same as the horizontal scale. No cross section is shown for the 1550 nm sample because there are no 3-D structures. The yellow arrow on 1550 nm image shows an area of a cluster that is still 2-dimensional but perhaps would have grown into a biofilm if allowed to grow for a longer period of time. Right column: SEM images of samples prepared in the same way as those shown on the left, but zoomed in to show detail of biofilm structures.

We quantify our results using the metric, relative coverage, which we define as follows:

$$\text{Relative Coverage (\%)} = \frac{\text{Fraction of colloidal crystals covered by biofilm}}{\text{Fraction of flat surface covered in biofilm}} \times 100\% \quad (1)$$

In our previous work, we show that our SEM sample prepartion dose not affect number and arrangement of the cells on the surfaces. So, the SEM images were used for the quantification purposes, and Figure 4 shows the image processing steps conducted using imageJ[53] software to calculate the area covered by biofilm structures. The average relative coverage is shown in Table 4-1, and the average fraction of the flat surface covered in biofilm is 0.16. The averages were derived from at least 12 different images (four images per each sample) with a total area of 2.71 mm2. Clearly, the colloidal crystals cause a large reduction in average coverage. Because the heights of the biofilms are irregular, it is difficult for us to compare biofilm volume on various samples, but the cross-sections in Fig. 4-4, show that the biofilms on the flat surfaces are thicker, so the colloidal crystals reduce the volume biofilm by even more than the data suggest in Table 4-1.

Table 4-1. Average relative coverage by 3D biofilm structures on various surface topographies. The average biofilm coverage on flat surfaces is 16%.

Substrate	**Flat**	**450 nm**	**1550 nm**
Relative coverage (% of flat coverage)	100	30 ± 20	13 ± 13
Average projected area of each biofilm (μm^2)	960 ± 430	620 ± 230	550 ± 160

Relative coverage does not provide information about the average size of a biofilm structure. We used the average area of the surface covered with a single 3D structure as a metric for the average size of a 3D structure. The results in Table 4-1 show the average area of one biofilm structure. Figure 4-5 shows the distribution of the size of the biofilm structures on the flat surface and colloidal crystals. The averages presented in the second row of table 1 are the average of the data presented in Fig. 4-5 after removing outliers. To remove outliers, data were sorted from small to large, and the first and last 20% of the data were treated as outliers. Table 4-1 shows that the average biofilm is smaller on the colloidal crystal, for example the biofilms are about half the size on the 1550 nm sample compared to the flat sample. Again, because the biofilms are thicker on the flat sample, the average volume would show a stronger trend than indicated in Table 4-1. Without removal of the outliers, the difference between the average area of each biofilm on 1550 nm spheres and flat surface is even larger.

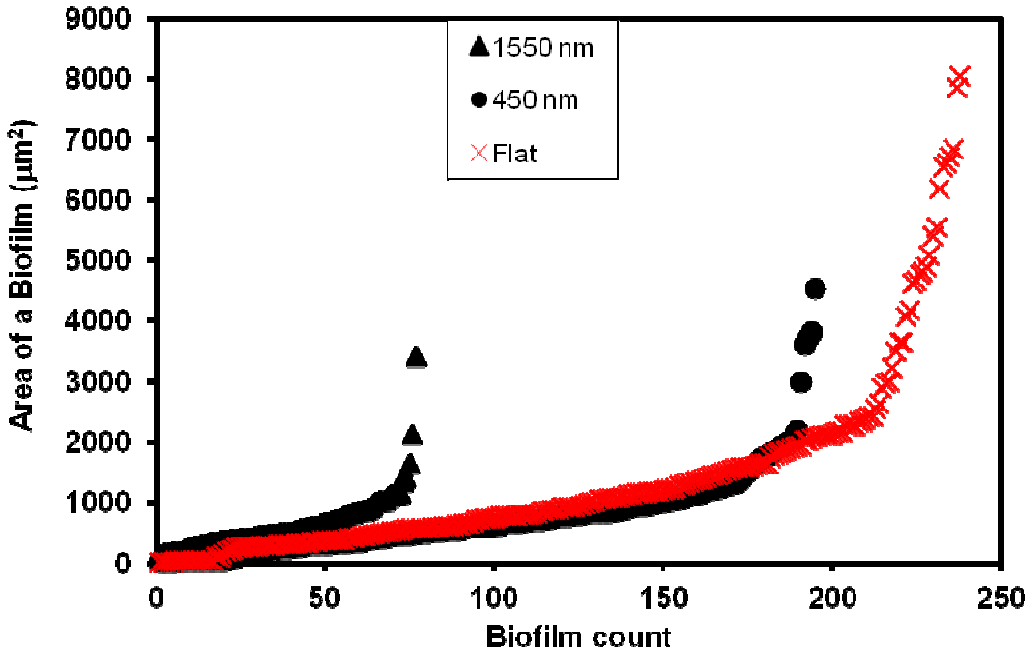

Fig. 4-5. The distribution of the average projected area of the 3D biofilm structures observed on flat surfaces and colloidal crystals. To calculate the numbers presented in the second row of table 1, these data were averaged after removing the outlier. The outlier is defined in the text.

In summary, both the 450 nm colloidal crystal and the 1550 nm colloidal crystal cause a significant reduction in the total volume of biofilm. The 1550 nm colloid produces larger reductions and therefore is more effective. It is possible that particles larger than 1550 nm would be even more effective. Since the flat sheet and the colloidal crystal layers are made from the same material (polystyrene), the results show that the reduction occurs due to the topography of the surface.

4-3-1-B. Effects of colloidal crystals on the single layer cell aggregation

After adhering to a surface, cells start forming single layer aggregations. As shown in Fig. 1-1, 3D (biofilm) structures arise from single-layer aggregations.[36]

Therefore, to understand the underlying mechanism by which colloidal crystals delay biofilm formation, we also examined cell aggregations that exist between the biofilm structures, and data from our prior work on one day experiments, which show the surface prior to biofilm formation.

Figure 4-6 represent a typical image of the cell aggregations after two days. Looking at images of the cell aggregations two main shapes of clusters are obvious: (1) high aspect ratio branches, and (2) larger clusters with low aspect ratio in which cells are densely packed. We used the word "*narrow clusters*" to refer to the first group. The term "*micro-colony*" was used to refer to the second group (See Fig. 4-6).-The arrangement of cell aggregations on the surfaces resulted in ring shape patterns in which an area of the solid surface is completely or partially surrounded by cell aggregations.

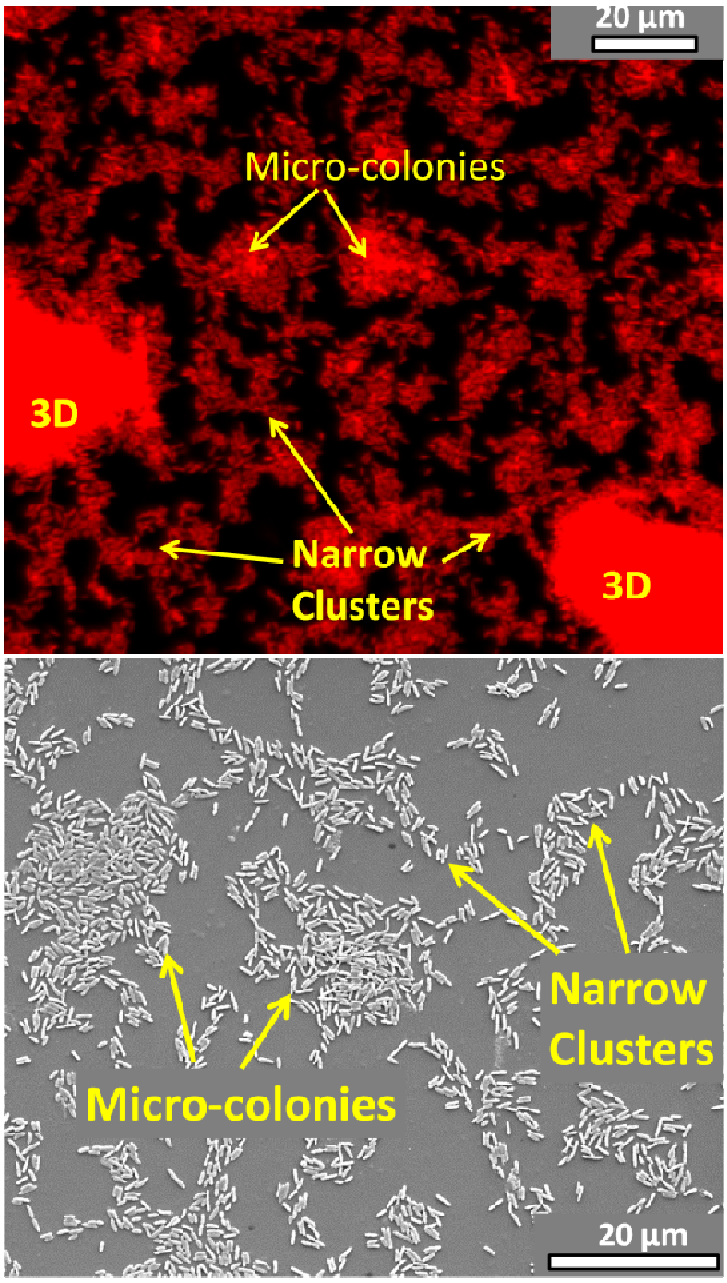

Fig. 4-6. Images of flat samples after two days showing narrow clusters, microcolonies and 3D structures (biofilm). Top: Fluorescent images acquired from the hydrated samples, Bottom: SEM image.

4-3-1-B-I. Colloidal Crystals can cause the alignment of bacteria within the cell aggregations.

Comparing the fluorescent images of the 1550 nm and flat samples one can see that the organization of the cells on the samples was affected by the colloidal crystal: the rod shaped bacteria have a preference to align with their long axis parallel to one of the three symmetry axes of the colloid crystal. This is made more clear by the two dimensional fast Fourier transform (FFT) of the image of the bacteria which is shown as an inset of fluorescent images in Fig. 4-7. The FFT shows the three preferred directions. In addition, the FFT of the 1550 nm crystal shows that there is a strong preference for a particular spacing between the cells. Comparison to the FFT of the colloidal crystal shows that the spacing and alignment is the same for the particles and the bacteria. However, there is not any clear alignment or spacing on flat or 450 nm samples.

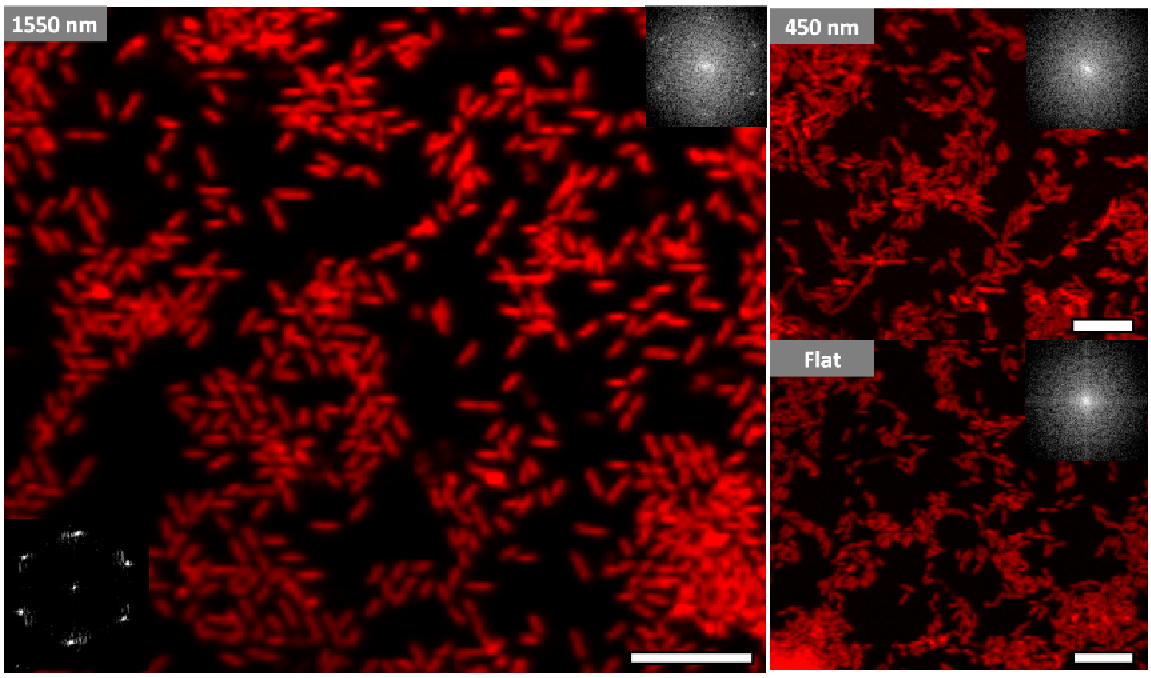

Fig. 4-7. Fluorescence images of *P. aeruginosa* attached to polystyrene with different surface topographies. Inset images on the top right corner show the FFT spectrum of each image. The

inset on left bottom corner of 1550 nm image shows the FFT spectrum of the particles behind the bacteria. All scale bars represent 10 μm.

4-3-1-B-II. Cell aggregations formed on 1550 spheres are non-touching

Figure 4-8A shows a typical SEM image of the cell aggregations on 1550nm colloidal crystals. Note that few cells touch another cell. This is true even in clusters (see e.g. B1). The majority of the cells selectively occupy confined spaces (See Fig. 4-1 for definition of a confined space). Evidently, individual confined spaces are too narrow to accommodate two cells, and adjacent confined-spaces are separated by too much distance to allow side by side body contact (See Fig. 2B for definition of the side). Visual inspection suggests that a higher fraction of contacts occur via the poles on the 1550 nm sample than on the flat sample.

Even though the bacteria on the 1550 nm sample make few preferential side-side body contacts with other bacteria, the bacteria still form aggregates. We use the term "*non-touching cluster*" to refer to such a collection of bacteria. This clusters on 1550nm colloidal crystal shares similar features to the narrow clusters observed on flat surfaces. Earlier work showed that a variety of micro-organisms, including *P. aeruginosa*, can be aligned by topographical features of the surface[14, 18, 22, 24-26, 29, 50, 51]. Here we show that despite this alignment, and despite the bacterial preference to be spaced apart on the crystals, *P. aeruginosa* still form aggregations on the crystals that are similar to those on a flat surface. This suggests that there is some communication or cooperative behavior between the bacteria over a distance.

As shown in Fig. 4-8A the majority of the 1550 nm colloidal crystals is covered by non-touching narrow clusters. However, our results show occasionally there are some

parts of aggregates that contains more touching cells (See Fig. 4-7). The fluorescent and SEM images presented in Fig. 6B and 6C compare a non-touching and a more-touching cluster. Figs. 4-8B and 4-8C show as the shape of the cluster changes from less populated narrow to dense and populated micro-colonies the clusters become more touching. The images show that on more populated clusters (Fig. 4-8C), there are several cells that could make body contact and align themselves with each other. This pattern is a well-known feature of cell-cell contact for rod shape microorganisms and believed to present mutli-cellualrity[61].

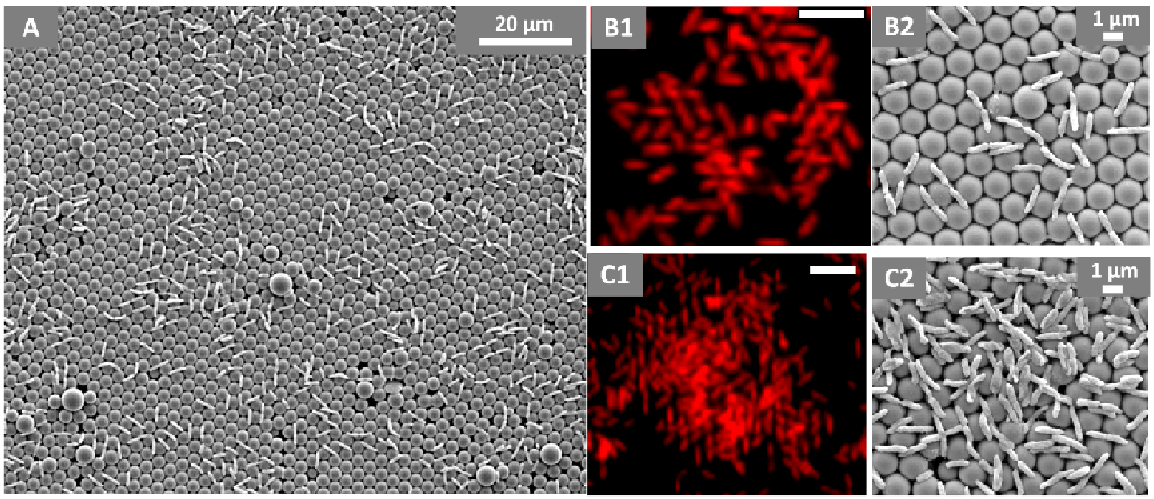

Fig. 4-8. A) Typical SEM image of aggregations formed by *P. aeruginosa* on 1550 nm colloidal crystals of polystyrene. B) B1 and B2 show non-touching narrow clusters in fluorescence and SEM images respectively. (C) C1 and C2 are showing a more populated micro-colony in fluorescent SEM images respectively. Scale bars on fluorescence images are 5 µm long. .

4-3-1-B-III. Cell aggregations are less dense on 1550 spheres dense than on 450nm spheres

Fig. 4-9 show SEM images cell aggregations on 450 nm spheres. Comparing Fig. 4-9A and 4-6A, it is evident that the cell aggression formed on 450 nm are more dense than those present on 1550nm. Fig. 4-9B is a high magnification SEM images of

P. aeruginosa adhered to 450nm particles. Fig. 4-9B shows that, although individual cells mainly aligned their body with one the three major axis of colloidal crystal, but there are several cells that could make side by side body contact and align themselves together. Also, Fig. 4-9B shows some cells that are contacting each other and they caused misalignments in the clusters.

Comparing the effects of 450nm and 1550nm on cell aggregation, it is concluded that 1550 nm particle will inhibit direct contact of the cells with crown for a longer period time and in higher extent. It also, caused delays in multicellular behavior of the cells represented by preferential contact of the cells. Therefore 1550nm particle, can delay formation of populated clusters and 3D biofilm structures for a longer period of time. In the next section we will provide results that show this conclusion is in agreement with our observations, when we run the experiment for shorter period of the time or with different nutrition condition.

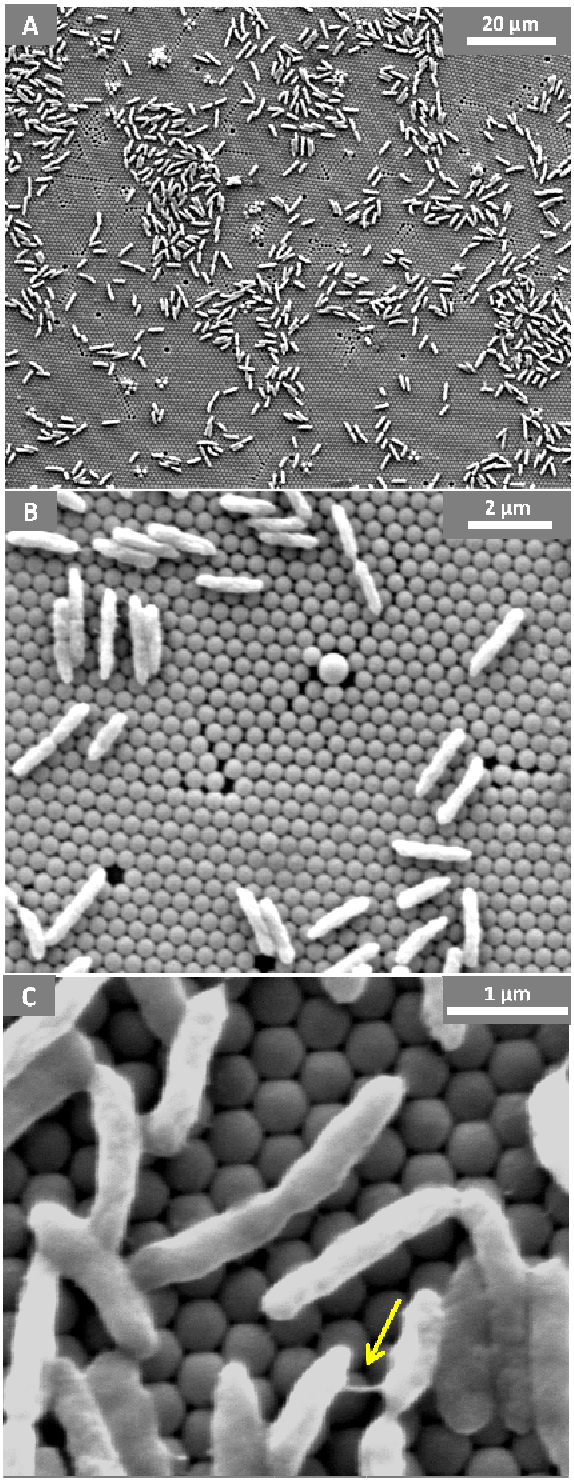

Fig. 4-9. A) Typical SEM images of the aggregations formed on 450nm spheres after two days. B abd C) High magnification SEM image of the cell aggregations on 450 nm colloidal crystals The arrow is referring to an appendage like structure which is connecting cells together.

4-3-2. The effect of the time and nutrition condition on the biofilm formation

In this section we will investigate the effect of time and nutrition on the formation and evolution of patterns on the colloidal crystals and flat surfaces. These results will help us to achieve a better understanding about the causes underlying the anti-biofilm properties of colloidal crystals.

Our previous work focused on one-day experiments in which conditions were the same as for the first day of the two-day experiments described here, so those one-day results tell us about the progression to the two-day state.[50] Results from the one-day experiments (Fig. 4-10) show that the flat surface is covered with narrow clusters, and there are 80% fewer cells on the 450 and 1550 nm colloidal crystals than on the flat surface. There are few clusters on the 450 nm crystals, each cluster has fewer bacteria, and the individuals within the cluster are not touching each other. There are no clusters on the 1550 nm colloidal crystal. The majority of the rare and small clusters are non-touching. During this first day, no clusters formed on the 1550 nm particles, and individual cells are rare. When bacteria do adsorb to the 450 and 1550 nm colloidal crystals, adsorption is primarily in the two-fold sites. For the 1550 nm colloidal crystal, the long axis of the rod-shaped bacteria are primarily oriented at 30° relative to the symmetry axis of the crystal (see Fig. 4-10). Thus, the arrangement of the bacteria is altered by the time/nutritional status: the shorter phenotype seen after one day sits mainly in the two fold side (bacterial axis 30° relative to a crystal axis), whereas the longer phenotype seen after two days sites mainly in the confined spacing (parallel to a crystal axis).

In this work, the experiment was run for a second day by feeding the reactor

with additional nutrient (100 mg/ml TSB). We conducted these experiments with one of two different flow rates: 5.2 ml/min, which we refer to as slower feeding or 10.5 ml/min, which we refer to as faster feeding. The first row of Figure 8 shows that for *flat PS*, even for slower feeding, the bacteria form microcolonies, and for the faster feeding they form a 3D biofilm, as described earlier in this paper. Some of the bacteria also change morphology over the second day (faster feeding): they become longer.

The second column of the Fig. 4-10 shows the results of the 2 days experiments with the slower feeding rate. The results for slower feeding show that the colloidal crystals slow the progression to micro colonies. There are no micro-colonies on the 1550 colloidal crystals and 450nm rarely supports formation of micro-colonies. There are some vague clusters on the 450 nm crystals. These clusters seems to be early stage narrow clusters. There are some small non-touching clusters on the 1550 nm crystals which are located far from each other. Most bacteria on the 1550 nm crystals avoid contact with each other and the crown, and they sit in the two-fold sites.

The third column summarizes the results of the two-day experiments with the faster feeding rate. As discussed earlier in this paper, the colloidal crystals hinder the formation of the 3D biofilm, and the larger, 1550 nm particles allowing fewer bacteria to adhere, and allow only non-touching clusters. So, regardless of whether the bacteria were fed slower or faster, the 1550 nm colloidal crystal are the best at delaying colony or biofilm formation.

Overall, comparing effect of the time and nutrition conditions on evolution of various patterns formed on flat and colloidal crystal coated surfaces I conclude that

colloidal crystals delay the colonization and biofilm formation, because they support biased presence of the cells on specific locations, ie. confined spaces. Over the time, cells start making contact with a previously adhered cells in the 2 fold sites while they are in contact with crown underneath. Comparing 1550 nm and 450nm spheres, we conclude that 1550 nm spheres are more efficient in delaying formation of biofilm, because they can hinder contact with larger crown for a longer period of time. In addition, 1550 nm spheres delay the second feature, adhesion to a bacteria and crown, for a longer period. Therefore 1550nm spheres perform better

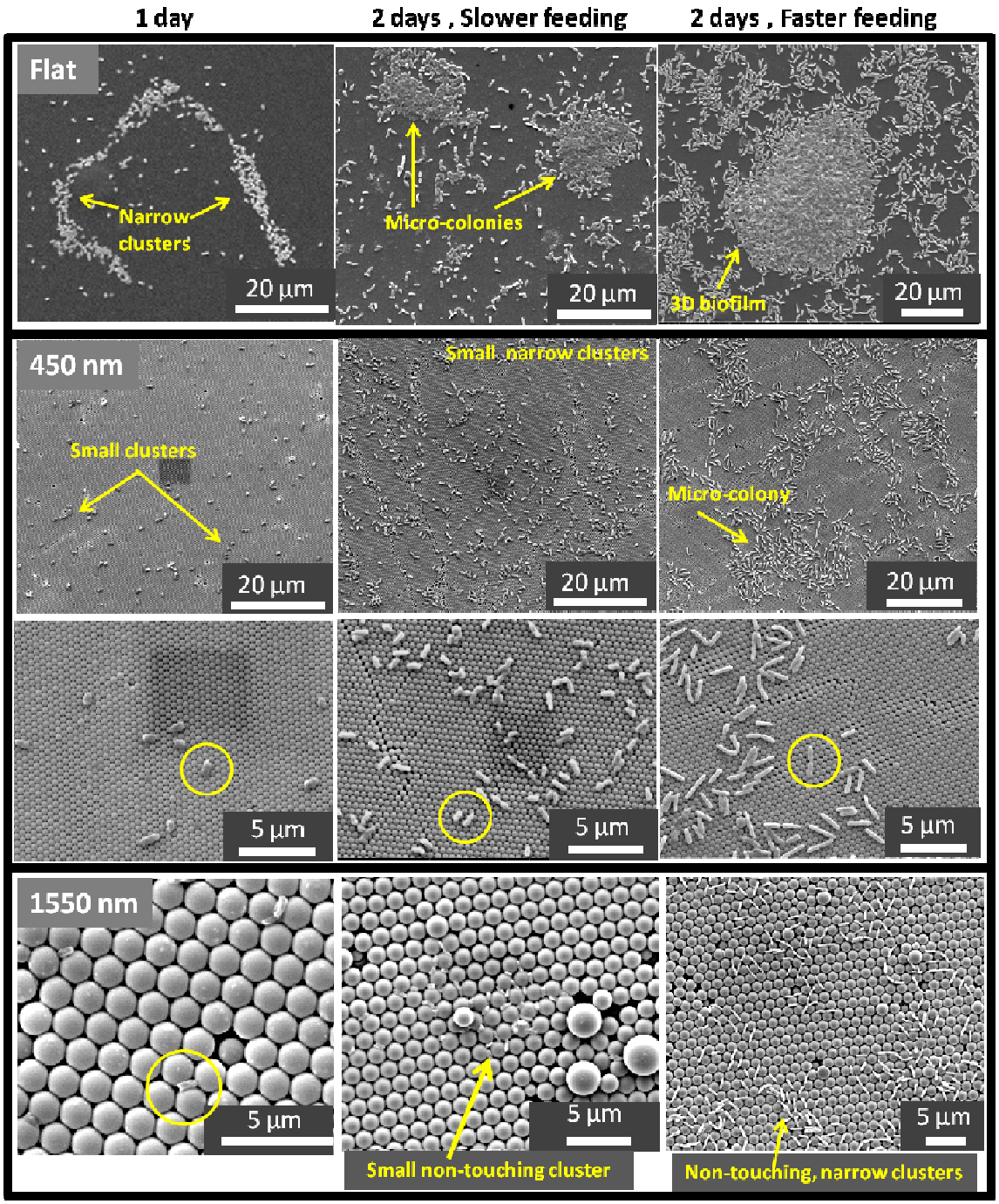

Fig. 4-10. SEM images of *P. aeruginosa* interacting with flat polystyrene or colloidal crystals of polystyrene. The first column shows the arrangement of the cells on surfaces after one day exposure to surfaces. The second and third column show the results of two day experiment for

two different nutrition condition as described in the text. The circles are referring to individual cells which are selectively adhered to the confined spaces.

4-4. Discussions

In this section, we will discuss how selective adhesion and formation of non-touching clusters may delay various stages of biofilm formation of *P. aerugniosa*. we will first discuss causes behind formation of non-touching clusters. Then we discuss a model which defines various stages of biofilm formation by *P. aeruginosa* on colloidal crystals. Finally, we will discuss the correlation between the arrangement of the cells and observed anti-biofilm properties.

4-4-1. Colloidal crystals support formation of non-touching colonies

The selective adhesion of the cells in specific areas or orientations of topographically engineered surfaces has been observed in past,[14, 18, 22, 24-26, 29, 50, 51] but (to the best of our knowledge) this is the first report showing that the larger-scale organization of the bacteria seen on flat surfaces can be approximately preserved while the cells remain with no body contact. Before explaining our thoughts on growth of non-touching clusters, we will briefly review previous observations and thoughts on the selective adhesion process.

4-4-1-A. Concept of selective adhesion to topographical engineered surfaces

In the discussion part of our previous work[50], we summarized the results of previous works on selective adhesion. In particular, we discussed the major works done by Scardino *et al.*[24, 25], Hochbaum and Aizenberg [18] and Kargar et. al[21, 22]. There has been several studies trying to understand and suggest a model to explain the selective

adhesion process. These works have been done using variety of microorganisms from marine microorganisms such as algae and diatoms[14, 24-26] to bacteria[18-22, 29, 30, 50, 51], specifically *P. aeruginosa*[18, 21, 22, 50]. In this studies, the topographical features of different shape has been made from variety of materials. In summary, previous observations suggest that microbes select positions on the surface which provides them with maximum contact area[18, 21, 22, 25, 50], however, this process may have some energy cost associated with deformation of the cell at the contact point[22]. Therefore, the binding site which provide less potential contact area or require more deformation upon contact are less favorable. The obsevation made by previous works suggest that surface motility of bacteria may provide the cells to explore different sites, ie. crowns or two fold sites, and bacteria might be able to distinguish less favorable area from the better ones[14, 21, 24, 50]. Also, if bacteria attaches to a less favorable area then their adhesion may not be strong enough, i.e reversible adhesion, and the shear forces may remove them from that area[14, 30, 50].

4-4-1-B. Formation of non-touching clusters and preferred alignments on 1550nm particles

When forming 2D aggregations on 1550nm spheres, each cell can be in contact with confined spaces, crown or another cell which was attached to one of the mentioned binding sites (See Fig. 4-11).

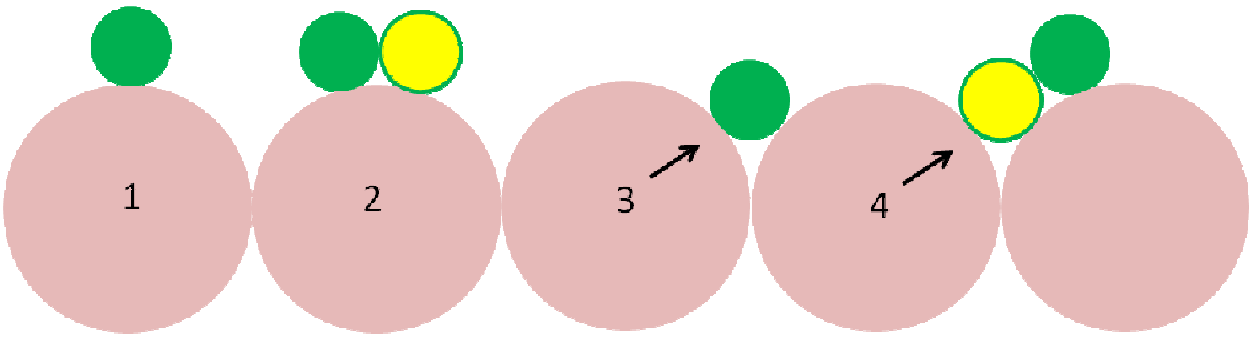

Fig. 4-11. Schematic showing adhesion possibilities available for a cell. The cell can contact 1) crown, 2) crown and a previously adhered cell to the crown, 3) confined space, 4) crown and a previously adhered cell to the confined space. The results shows that 3 is the preferred contact. Colloidal crystals are shown in larger red circles, new bacteria in green and previously attached cells in yellow.

The results indicate that contact with confined spaces is the first priority for making contact with surface. This priority results in the presence of single cells during the first day. This could be because adhering to a single sphere will only provide one contact point for rod shape cells and increasing the contact area requires deformation of the cells which is not favorable. However being in confined spaces cells can contact multiple spheres and consequently, making similar contact area would require much less local deformation. The geometry of 1550nm sphere provides confined spaces that can support presence of only one rod shape *P. aerugnisa* cell (typical diameter of the cells is between 500-600nm). Therefore, as long as cells prefer to stay in touch with solid surface, i.e do not pile up on each other, then formation of contact with a cell which is already located within the confined spaces, reduces the chance of the second cell to make contact with multiple spheres. If the gains associated with making cell-cell body contact is more than the costs associated with lose of cell-surface contact then the cell-cell contact would be preferred. This gain could be both biological and thermodynamic driven. The biological gains may benefit individual cells and/or the society of the microbes. The thermodynamic driven gain could be the gain in adhesion energy due to more cell-cell contact. Formation of non-touching clusters indicate that the gains

associated with cell-cell contact are not enough to counter-balance the costs associated with cell-sphere contact. Therefore, as the cluster grows, the cells will occupy more confined spaces which are hexagonally arranged on the colloidal crystals. The hexagonal arrangement, provides three major axis therefore we observed this alignment on Fig. 4-7.

4-4-2. Non-touching arrangement delays all steps of biofilm formation process

4-4-2-A. The same model may explain development of biofilm on flat and colloidal crystals surface

As discussed previously, biofilm formation process is composed of several stages from reversible adhesion to formation of mature 3D biofilm (Figure 1-1). Comparing the effect of time and nutrient condition on development of biofilm on surfaces, suggest that *P. aeruginosa* goes through similar stages on all samples, however colloidal crystals causes delays and affects some arrangement of the cells on the surface. Our results suggest that biofilm formation is composed of four consecutive stages : 1- adhesion of the cells to the surfaces, 2- formation and growth of narrow clusters 3- formation and growth of micro-colonies and 4- formation and growth of 3D structures of biofilm. Small clusters observed on 450nm (1 day) and 1550nm (after a second day of slower feeding) could be interpreted as an intermediate stage between the first and the second stages.

4-4-2-B. First stage, adhesion

The one-day results shows that flat surfaces support both cell-surface and cell-cell contact (formation of narrow colonies). This observation indicates that the cells are irreversibly attached to the flat surface as they could start forming clusters. However, the cells selectively adhere to the confined spaces of 1550nm spheres and they neither make direct cell-cell contact nor form non-touching colonies. This might be because changing

the from reversible adhesion to irreversible may take longer and consequently delays cluster formation.

Lack of non-touching clusters, may indicate that selective adhesion to 1550nm particles, not only delayed cell-cell interactions which require direct cell-cell body contact, but also, the cell-cell interactions such as quorum sensing which do not rely on body-contact. 450 nm spheres reduced the number of adhered cells to the same extent as 1550nm (80% reduction)[50]. They also supported the selective adhesion process. However, 450 nm support formation of small colonies[50]. We interpret that selective adhesion to 450 nm also delays irreversible adhesion process however in less extent than 1550 nm. Therefore some cells transited to the irreversible adhesion and start forming clusters. This could be due to the less distance between two nearby parallel 2-fold sites, which is equal to diameter of spheres. Therefore, on 450 nm, the cells can be in touch with both confined spaces and the second cells and take the advantage of the benefits from both side. As discussed previously, for both particle sizes, selective adhesion to confined spaces provides more contact points and therefore the selective adhesion process observed in both[50]. Also, it should be mentioned that sometimes cells are not exactly aligned with the direction of two-fold-sites. This little misalignment may help the cells to gain the optimal arrangement with maximum contact area. We discussed the possible reason behind observation of statistically independent adhesion density on 1550nm and 450 nm particles in the previous chapter of dissertation [50]. Briefly, despite 450nm particles provide more contact points, each contact point may support less deformation of the cells, due to the curvature effect[22]. Therefore the total area of contact could be similar which results in similar adhesion density.

4-4-2-C. Second stage, formation of narrow clusters

Analyzing the images show that narrow clusters are the second structures that evolve after bacteria adhered to the surfaces. This stage happens on flat surfaces within the first day. However, the experiments need to be run for the second day (regardless of nutrient condition) to support formation of narrow clusters from cells which are selectively adhered to 450nm spheres. Slower flow rate supports formation of the small non-touching clusters on 1550nm spheres. This observation supports our hypothesis that considered formation of small clusters as an intermediate stage between adhesion and narrow cluster formation. These non-touching clusters can act as nucleation foci for formation of non-touching narrow clusters. When the growth of the cells is supported by faster feeding of the nutrient, narrow clusters will develop and become the dominant structures on 1550nm sphere, albeit majority of them are non-touching.

This observation suggests that, individual cells prefer direct contact with two fold sites, however their collection benefits from formation of narrow clusters. Preference of the cells to the confined spaces results in less cells on the surfaces, and delays irreversible adhesion. This will cause formation of less small clusters, which are nucleation point for formation of narrow clusters. It also results in the non-touching arrangement. The reduced number of the cells and the non-touching arrangement can reduce the various types of cell-cell communication. The formation of non-touching narrow clusters indicates that the biological causes of this phenomenon might be less dependent on the direct cell to cell and be more depended on the number of the cells. The narrow clusters formed here share some similarities with the rafts observed in swarm motility of bacteria[62, 63]. In an hypothetical model, Shrout et. al. [34] suggested that swarm

motility of bacteria may play a role in formation of clusters by *P. aeruginosa.* It is already known that quorum sensing affects the swarm motility[34]. Therefore, observation of narrow clusters may have some relationships with swarm motility, e.g. swarming is acting as a motility mode and probably is the dominant mode. The reduced number of the cells on the surface may delay/alter some parts of quorum sensing process and consequently delays swarming and formation of narrow clusters. Analysis of this hypothesis and understanding the phenomena of course requires further experiments.

4-4-2-D. Third stage, formation of micro-colonies

Flat surface support formation of micro-colonies during the second day (regardless of nutrient condition). This structure will eventually evolve on both 450nm and 1550nm spheres however, they require faster nutrient flow. 450nm spheres rarely support formation of these structures during the lower nutrient flow as well. Comparing to 450nm, 1550 nm supports formation of less micro-colonies during the faster flow rate conditions. This can be interpreted as the delay in micro colony formation.

Presence of the rare more-touching and packed micro-colonies on 1550 nm particles shows that the cells will finally start touching each other. This means that at this stage, the benefits gained from cell-cell contact will be large enough to overcome the potential losses due to poor contact with the unfavorable positions on the particle, such as the crown.

Lack of body contact can negatively affect several biological process. For example, it is known that bacteria can directly make contacts using their appendages[64] to communicate. Fig. 4-7 shows a contact made between cells using their appendages.

Bacteria may use these processes to transfer genetic information to other cells[64] Therefore the space created between nearby cells due to reduced body contact may reduce the number of cell-cell contact throughout appendages and negatively affect biological activities of the cells within the clusters. Therefore, the direct body contact can reduce this loss. Previously, it was discussed that the strong adhesion of the cells to each other may result in creation of intercellular matrix which can arrest the cell motility[34]. down-regulation of motility is required for formation of micro-colonies [34] therefore cell-cell contact can create a value for the micro-colony. There might be several other potential factors that non-touching arrangement delays them, however understating them requires further studies.

4-4-2-E. Third stage, formation of 3D structures

This stage only happens when the experiments ran for two days and the reactor gets fed at faster nutrient flow. The analysis show that both colloidal crystals support formation of t3D structures less than flat, and 1550nm spheres show the minimum coverage. Therefore it can be interpreted that 1550 nm spheres caused the maximum delay in formation of 3D biofilm structures. The results here could be interpreted as early stage biofilm in which the cells are forming the stalk of the mushrooms as described by Klausen et, al.[34] for bacteria fed with glucose as was used here [31, 35].

4-5. Conclusions

We compared interactions of *P. aeruginosa* with both flat surfaces of polystyrene and surfaces coated with a monolayer of close-packed spheres. We conclude that colloidal crystals delay the initial adhesion, the organization into microcolonies, and

the formation of biofilms. Delays in both colonization and biofilm formation processes are greater for spheres of greater diameter (1550 nm vs 450 nm). Furthermore, the distribution of *P. aeruginosa* over the colloidal crystal is not homogeneous or isotropic: the bacteria are aligned in one of three directions and mainly sit in the confined spaces. We propose that the delay of biofilm is caused by the selective adhesion. Although the colloidal crystal provides some (preferred) adhesion sites, the spacing between these preferred sites enforces separation between the adhered bacteria. We propose that the greater separation between bacteria, and possibly the arrangement, hinders the formation of a biofilm. Although the colloidal crystal alters the local arrangement of cells on the scale of the bacteria, and greatly reduces the area in which the bacteria touch each other, the bacteria still form clusters on the colloidal crystal. We have described these clusters as "non-touching" colonies; evidently there is still a preference for colonies even when the cells are not touching. The bacteria are able to bridge between the favorable sites on the smaller spheres (450 nm) within two days, but not on the larger particles (1550 nm). The bridges occur in the middle of a colony, and there is some progression to 3D structures (biofilms).

.

Chapter 5. Summary

5-1. Conclusions

We compared interactions of *P. aeruginosa* with both solid surfaces and surfaces coated with colloidal crystals of polystyrene. We conclude that geometrical conditions provided by assembly of particles creates special geometrical conditions that delay all the stages of biofilm formation process from adhesion to biofilm formation. This special geometry is composed of a curved crown and the confined spaces between the nearby particles.

Studying the adhesion and early stage cluster formation, it was observed that (1) the colloidal crystal reduced the number density of bacteria adhered to the surface by about 80% for particle diameters in the range 450–1550 nm; (2) assembly of spheres with diameters in the range 220–1550 nm reduced the incidence of cluster formation, and no clusters were observed. For longer-term experiments, the delays in both colonization and biofilm formation processes increase as the particle diameter increases. It is possible that particles larger than 1550 nm would be even more effective.

For particle diameters exceeding 450 nm, *P. aeruginosa* selectively adhere in the confined spaces (i.e. two-fold and three fold sites) and are rarely found on the particle crown during the adhesion and early cluster formation (in one day experiments here). During the colony growth and early stage 3D biofilm formation stages (in two days experiments here), *P. aeruginosa* still exhibits selective adhesion, the bacteria are aligned in one of three directions and mainly sit in the confined spaces. The results prove that the organization of the bacteria into colonies is affected by the colloidal crystals: they

form non-touching colonies with preferred alignments on the surface.

We propose that the delay of biofilm is caused by the selective adhesion. Bacteria do not prefer to be in contact with crown, therefore any assembly of particles with appropriate size, reduces the potential binding sites on the surface. The spacing between these preferred sites enforces separation between the adhered bacteria. The greater separation between bacteria hinders their formation of a biofilm. This principle, may be used to design other topographical features for anti-fouling applications.

Our results are consistent with the idea that it is more difficult for bacteria to adsorb to curved surfaces, and that bacteria select between different surface sites based on the local geometry. Furthermore, the results are consistent with the idea that the formation of colonies can be influenced by the proximity of favorable adsorption sites for individual bacteria. The results presented in the appendix 1 suggest that colloidal crystals can also delay adhesion of *Methicillin resistant staphylococcus aureus* (MRSA) while it supports selective adhesion of this bacterium to the confined spaces. The incidence of bacterial colony formation on a medical grade stainless steel needle (diameter = 1.5 mm) was reduced by coating it with 450 nm particles. This result suggests that application of particle assembly is a promising strategy to delay adhesion and colony formation of microbes on a variety of materials and geometries.

5-2. Major contributions to the field

This dissertation introduces assembly of spherical particles as a novel topography-based antibiofouling coating. It also provides new insights on the effects of surface topography, especially local curvature, on cell–surface and cell–cell interactions during the evolution

of biofilms. Our results are consistent with the idea that it is more difficult for bacteria to adsorb to curved surfaces, and that bacteria select between different surface sites based on the local geometry. Furthermore, the results are consistent with the idea that the formation of colonies can be influenced by the proximity of favorable adsorption sites for individual bacteria.

The major contributions of the third chapter were published in Journal of Materials Chemistry B. The major conclusions are:

- The colloidal crystal-coating reduces the number density of *P. aeruginosa* adhered to the surface, reduces the number of microbial colonies, and alters the arrangement of the cells. In particular:
    - The colloidal crystal reduced the number density of bacteria adhered to the surface by about 80% for particle diameters in the range 450–1550 nm
    - Spheres with diameters in the range 220–1550 nm reduced the incidence of colony formation, and no colonies were observed when the particle diameter was in the range 630–1550 nm.
    - For particle diameters exceeding 630 nm, *P. aeruginosa* selectively adhere in the 2-fold sites and are rarely found on the particle crown.
- The incidence of bacterial colony formation on a medical grade stainless steel needle (diameter = 1.5 mm) was reduced by coating it with 450 nm particles. This result suggests that application of a layer of colloidal particles is a promising strategy to delay adhesion and colony formation of microbes on a variety of materials and

geometries.

The major contributions of the fourth chapter are prepared to be submitted as a Journal publication. I studied the effect of colloidal crystals on biofilm formation of *P. aeruginosa.* The major conclusions are:

- Colloidal crystals delay all the stages of biofilm formation process from adhesion to biofilm formation.

- Delays in both colonization and biofilm formation processes is greater for particles of greater diameter (1550 nm vs 450 nm).

- *P. aeruginosa* still exhibits selective adhesion over two days: the bacteria are aligned in one of three directions and mainly sit in the confined spaces.

- The results prove that the organization of the bacteria into colonies is affected by the colloidal crystals: they form non-touching colonies.

- I propose that the delay of biofilm is caused by the selective adhesion. Although the colloidal crystal provides some (preferred) adhesion sites, the spacing between these preferred sites enforces separation between the adhered bacteria. The greater separation between bacteria hinders their formation of a biofilm. The delay in adhesion as well as the arrangement of the adherent bacteria and possible causes of the delay in colony formation and biofilm formation

The results presented in the appendix A suggest that colloidal crystals may also delay adhesion of *Methicillin resistant staphylococcus aureus* (MRSA) while it supports

selective adhesion of this bacterium to the confined spaces.

5.3. Suggestions for future works

In this dissertation, I explained several potential effects of the particle coating on cell-surface and cell -cell interactions. For example I hypothesized that particles may up-regulates the cell motility or delays down regulation of cell motility. The live imaging of the cell-surface and cell-cell interaction would be certainly suggested as the first future step to understand these phenomena. One interesting experiment would be creating colloidal crystals of a variety of sizes on one sample and study the cell-surface interactions. This experiment may provide new insights about the exploratory behavior of bacterial cells when interacting with topographically engineered surfaces. Also, I provided insights on the potential effect of the surface curvature on bacteria-surface interaction, however future works are required to understand the phenomena. Further theoretical analysis of the interactions of bacteria with surface topography would be an important next stage toward better understanding the phenomena. In particular, non-dimensional analysis of the experimental results might provide new insights about the effects of the curvature on the biofilm formation on topographically engineered surfaces

In this dissertation, I proved that assembly of particles can act efficiently as a topographical based anti-biofilm coating. However, there is still room for further technological development of the idea. For example by functionalizing the particles or increasing the durability of the coating. I included two suggestions with further details in appendix B.

References

1. R. M. Klevens, J. R. Edwards, C. L. Richards, T. C. Horan, R. P. Gaynes, D. A. Pollock and D. M. Cardo, *Public Health Rep.*, 2007, **122**, 160-166.
2. J. D. Bryers, *Biotechnol. Bioeng.*, 2008, **100**, 1-18.
3. A. Geddes, *Journal of Antimicrobial Chemotherapy*, 2000, **46**, 873-877.
4. P. S. Stewart and J. W. Costerton, *Lancet*, 2001, **358**, 135-138.
5. F. FitzGerald, J. O'Gorman, M. M. Morris-Downes, R. K. Crowley, S. Donlon, R. Bajwa, E. G. Smyth, F. Fitzpatrick, P. J. Conlon and H. Humphreys, *Journal of Hospital Infection*, 2011, **79**, 218-221.
6. M. Blaser, *Nature*, 2011, **476**, 393-394.
7. I. Banerjee, R. C. Pangule and R. S. Kane, *Advanced Materials*, 2011, **23**, 690-718.
8. A. Marmur, *Biofouling*, 2006, **22**, 107-115.
9. P. Ball, *Nature*, 1999, **400**, 507-+.
10. C. Baum, W. Meyer, R. Stelzer, L. G. Fleischer and D. Siebers, *Marine Biology*, 2002, **140**, 653-657.
11. A. Scardino, R. De Nys, O. Ison, W. O'Connor and P. Steinberg, *Biofouling*, 2003, **19**, 221-230.
12. A. V. Bers and M. Wahl, *Biofouling*, 2004, **20**, 43-51.
13. K. Anselme, P. Davidson, A. M. Popa, M. Giazzon, M. Liley and L. Ploux, *Acta Biomaterialia*, 2010, **6**, 3824-3846.
14. M. E. Callow, A. R. Jennings, A. B. Brennan, C. E. Seegert, A. Gibson, L. Wilson, A. Feinberg, R. Baney and J. A. Callow, *Biofouling*, 2002, **18**, 237-245.
15. K. K. Chung, J. F. Schumacher, E. M. Sampson, R. A. Burne, P. J. Antonelli and A. B. Brennana, *Biointerphases*, 2007, **2**, 89-94.
16. C. Díaz, P. L. Schilardi, P. C. dos Santos Claro, R. C. Salvarezza and M. n. A. Fernández Lorenzo de Mele, *ACS applied materials & interfaces*, 2009, **1**, 136-143.
17. A. K. Epstein, A. I. Hochbaum, P. Kim and J. Aizenberg, *Nanotechnology*, 2011, **22**.
18. A. I. Hochbaum and J. Aizenberg, *Nano Letters*, 2010, **10**, 3717-3721.
19. S. Y. Hou, H. A. Gu, C. Smith and D. C. Ren, *Langmuir*, 2011, **27**, 2686-2691.
20. L. C. Hsu, J. Fang, D. A. Borca-Tasciuc, R. W. Worobo and C. I. Moraru, *Appl. Environ. Microbiol.*, 2013, **79**, 2703-2712.
21. M. Kargar, A. Kim, A. S. Nain and B. Behkam, in *Annual Meeting of Adhesion Society*, Daytona Beach, FL, USA, 2013.

22. M. Kargar, J. Wang, A. S. Nain and B. Behkam, *Soft Matter*, 2012, **8**, 10254-10259.

23. E. Kim, W. H. Kinney, A. R. Ovrutsky, D. Vo, X. Bai, J. R. Honda, G. Marx, E. Peck, L. Lindberg and J. O. Falkinham, *FEMS microbiology letters*, 2014.

24. A. J. Scardino, J. Guenther and R. de Nys, *Biofouling*, 2008, **24**, 45-53.

25. A. J. Scardino, E. Harvey and R. De Nys, *Biofouling*, 2006, **22**, 55-60.

26. J. F. Schumacher, M. L. Carman, T. G. Estes, A. W. Feinberg, L. H. Wilson, M. E. Callow, J. A. Callow, J. A. Finlay and A. B. Brennan, *Biofouling*, 2007, **23**, 55-62.

27. J. F. Schumacher, C. J. Long, M. E. Callow, J. A. Finlay, J. A. Callow and A. B. Brennan, *Langmuir*, 2008, **24**, 4931-4937.

28. R. Vasudevan, A. J. Kennedy, M. Merritt, F. H. Crocker and R. H. Baney, *Colloids and Surfaces B: Biointerfaces*, 2014, **117**, 225-232.

29. K. A. Whitehead, J. Colligon and J. Verran, *Colloids and Surfaces B-Biointerfaces*, 2005, **41**, 129-138.

30. L. C. Xu and C. A. Siedlecki, *Acta Biomaterialia*, 2012, **8**, 72-81.

31. P. K. Singh, M. R. Parsek, E. P. Greenberg and M. J. Welsh, *Nature*, 2002, **417**, 552-555.

32. S. L. Gellatly and R. E. W. Hancock, *Pathog. Dis.*, 2013, **67**, 159-173.

33. J. D. Shrout, D. L. Chopp, C. L. Just, M. Hentzer, M. Givskov and M. R. Parsek, *Molecular microbiology*, 2006, **62**, 1264-1277.

34. M. Klausen, A. Aaes-Jørgensen, S. Molin and T. Tolker-Nielsen, *Molecular microbiology*, 2003, **50**, 61-68.

35. L. Lorenz, B.-M. K and G. D, in *Montana Biofilm Science & Technology Meeting*, Montana State University Center for Biofilm Engineering, Bozeman, MT, USA, 2013, p. 26.

36. G. M. Patriquin, E. Banin, C. Gilmour, R. Tuchman, E. P. Greenberg and K. Poole, *Journal of bacteriology*, 2008, **190**, 662-671.

37. U. Seifert and R. Lipowsky, *Phys. Rev. A*, 1990, **42**, 4768-4771.

38. E. Sackmann and R. F. Bruinsma, *ChemPhysChem*, 2002, **3**, 262-269.

39. M. Retsch, Z. C. Zhou, S. Rivera, M. Kappl, X. S. Zhao, U. Jonas and Q. Li, *Macromolecular Chemistry and Physics*, 2009, **210**, 230-241.

40. J. T. Zhang, L. L. Wang, D. N. Lamont, S. S. Velankar and S. A. Asher, *Angewandte Chemie-International Edition*, 2012, **51**, 6117-6120.

41. N. Vogel, S. Goerres, K. Landfester and C. K. Weiss, *Macromolecular Chemistry and Physics*, 2011, **212**, 1719-1734.

42. A. M. Brozell, M. A. Muha, B. Sanii and A. N. Parikh, *Journal of the American Chemical Society*, 2006, **128**, 62-63.

43. Y. H. Wang and W. D. Zhou, *Journal of Nanoscience and Nanotechnology*, 2010, **10**, 1563-1583.

44. Z. C. Lu and M. Zhou, *Journal of Colloid and Interface Science*, 2011, **361**, 429-435.

45. W. L. Bragg, in *Proceedings of the Cambridge Philosophical Society*, 1913, p. 4.

46. R. J. Hunter, *Foundations of Colloid Science*, Oxford University Press, Oxford, 1987.

47. J. Chandra, P. K. Mukherjee and M. A. Ghannoum, *Nature Protocols*, 2008, **3**, 1909-1924.

48. D. M. Goeres, L. R. Loetterle, M. A. Hamilton, R. Murga, D. W. Kirby and R. M. Donlan, *Microbiology-Sgm*, 2005, **151**, 757-762.

49. K. Buckingham-Meyer, D. M. Goeres and M. A. Hamilton, *Journal of Microbiological Methods*, 2007, **70**, 236-244.

50. M. Kargar, A. Pruden and W. A. Ducker, *Journal of Materials Chemistry B*, 2014, **2**, 5962-5971.

51. C. Diaz, P. L. Schilardi, R. C. Salvarezza and M. F. L. de Mele, *Langmuir*, 2007, **23**, 11206-11210.

52. E. Medilanski, K. Kaufmann, L. Y. Wick, O. Wanner and H. Harms, *Biofouling*, 2002, **18**, 193-203.

53. C. A. Schneider, W. S. Rasband and K. W. Eliceiri, *Nat. Methods*, 2012, **9**, 671-675.

54. C. Gomez-Suarez, H. J. Busscher and H. C. van der Mei, *Appl. Environ. Microbiol.*, 2001, **67**, 2531-2537.

55. P. Singleton and D. Sainsbury, in *Dictionary of Microbiology and Molecular Biology*, John Wiley & Sons, Ltd, 2007, pp. 451-508.

56. K. Hori and S. Matsumoto, *Biochem. Eng. J.*, 2010, **48**, 424-434.

57. C. M. Waters and B. L. Bassler, in *Annual Review of Cell and Developmental Biology*, Annual Reviews, Palo Alto, 2005, pp. 319-346.

58. J. W. Costerton, P. S. Stewart and E. P. Greenberg, *Science*, 1999, **284**, 1318-1322.

59. E. Kim, W. H. Kinney, A. R. Ovrutsky, D. Vo, X. Bai, J. R. Honda, G. Marx, E. Peck, L. Lindberg, J. O. Falkinham, R. M. May and E. D. Chan, *FEMS Microbiology Letters*, 2014, **359**, 1-6.

60. E. P. Ivanova, J. Hasan, H. K. Webb, V. K. Truong, G. S. Watson, J. A. Watson, V. A. Baulin, S. Pogodin, J. Y. Wang, M. J. Tobin, C. Lobbe and R. J. Crawford, *Small*, 2012, **8**, 2489-2494.

61. J. A. Shapiro, *Annual Reviews in Microbiology*, 1998, **52**, 81-104.

62. T. Köhler, L. K. Curty, F. Barja, C. van Delden and J.-C. Pechère, *Journal of bacteriology*, 2000, **182**, 5990-5996.

63. M. H. Rashid and A. Kornberg, *Proceedings of the National Academy of Sciences*, 2000, **97**, 4885-4890.

64. J. W. Schertzer and M. Whiteley, *Cell*, 2011, **144**, 469-470.

65. H. J. Nam, D.-Y. Jung, G.-R. Yi and H. Choi, *Langmuir*, 2006, **22**, 7358-7363.

66. D. D. Iarikov, M. Kargar, A. Sahari, L. Russel, K. T. Gause, B. Behkam and W. A. Ducker, *Biomacromolecules*, 2013, **15**, 169-176.

Appendix A. Colloidal Crystals can delay adhesion of *Methicillin resistant staphylococcus aureus* (MRSA)

Using the one-day CDC reactor assay, I tested effects of the colloidal crystals on the adhesion of MRSA to the surface. The preliminary results, suggest that colloidal crystals can 1) delay adhesion of MRSA to the surface and 2) support selective adhesion of MRSA to the confined spaces. Before making any further conclusions, It is recommended to run longer time experiments. Considering similarities in shape of MRSA with spheres, it is recommended that fluorescent images get used or further quantitative analysis.

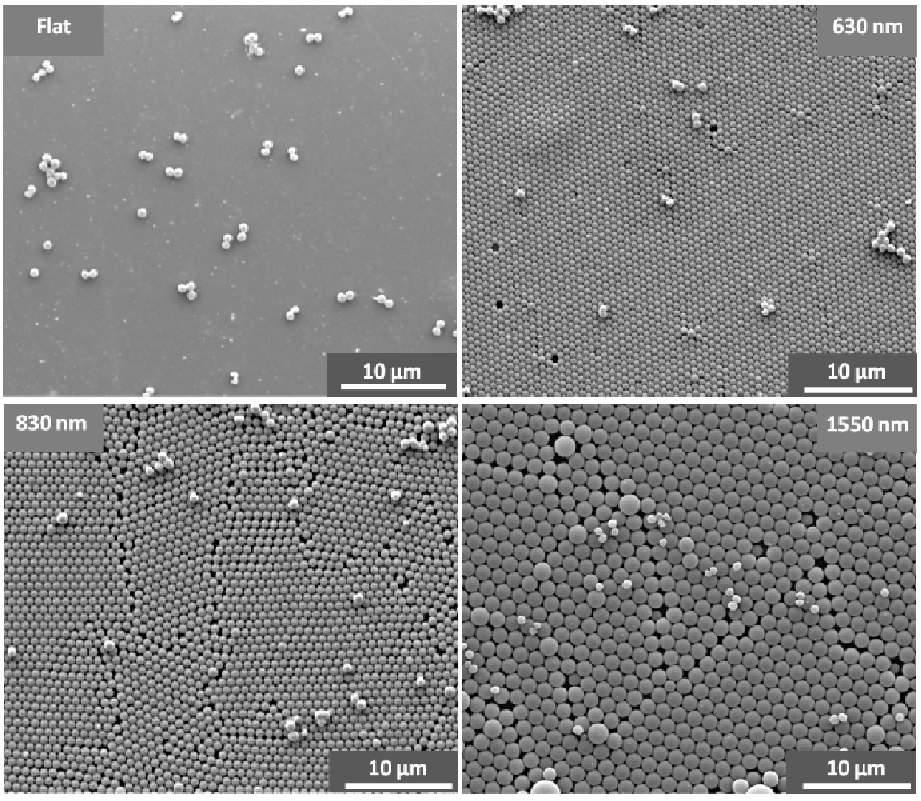

Fig. A-A-1. SEM images of MRSA cells interacting with flat and colloidal crystals. The number of the cells 1550nm particles may not be representative

.

Appendix B. Suggestions for Future Works

A-B-1. Topographical Antifouling Material from a Mold

An alternative to coating devices with particles is to include the topography in the original part. One method of doing this is to use our coating in the manufacture of a mold. The mold is then used for the manufacture of the final part[65]. Figure A2-1 shows how the final part (green part shown in step 5) can be produced from a mold (pink part in 2) that is itself made using the colloidal crystal as a template. The advantage of the mold is that (a) the colloidal crystal need only be made once to make many parts and (b) the final part can be made from a material that might be difficult to produce particles from. For example the final part could be made from polydimethylsiloxane (PDMS) whereas it is difficult to make particles from this material. The other advantage is that it might be cheaper or fast to make many parts from a mold.

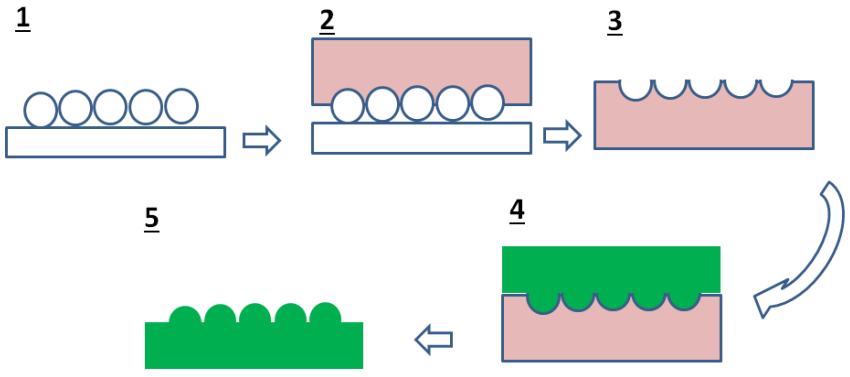

Fig. A-B-1. Texturizing surfaces by molding: 1-Texturizing surfaces with particles, 2-Molding the red material on particles, 3-Removing particles. This can be a considered as a textured surface itself or functions as a secondary mold 4-Deposition of the appropriate material in secondary mold, 5- Removing the secondary mold and texturizing the final material.

A-B-2. Combined chemical-topographical coatings for prevent microbial colonization of materials

A-B-2-1. Principles

Chemistry can be combined with chemical approaches. In the combined approach, engineered geometry *delays adhesion* of the microbes to the surface (**Anti-adhesion**), while chemical modification of the surface is applied to kill the bacteria upon contact (**Anti-micriobial**). The geometrically-induced reduction in adhesion strength of the cells to the surface means that the body of dead cells will be released easily which will lead to the long term efficacy of the chemical coating.

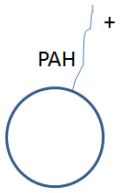

Fig. A-B-2. Particle coated surfaces (or molded) can be functionalized using molecules such as Polyallylamine (PAH) which are known to kill bacteria upon contact[66].

A-B-2-2. Antibacterial-antiadhesion topographical coating

In this approach the molecules that are known to kill bacteria in contact will be added to our topographical features. This can be our previously developed Polyallylamine coating which kills bacteria[66] by disrupting the bacterial cell membrane, which is a separate mechanism from antibiotics, and thus is also not subject to antibiotic resistance. We want to make our molded textures from silicone rubber and then functionalize them with molecules which kills cells upon contact. The chemistry can be a results of other materials which may act through a similar or different mechanism